

**bg-2017-83**

**Changes in the partial pressure of carbon dioxide in the Mauritanian-Cape Verde upwelling region between 2005 and 2012**

Melchor González-Dávila, J. Magdalena Santana Casiano, and Francisco Machín

Following the editor instructions and the two reviewer's comments we have considered all the indications in order to achieve the Biogeosciences standards of quality in its publications.

We have answered all the points asked by the reviewers and the text has been changed in order to include the improvements indicated by the reviewers. The abstract has been modified, the text has been checked by a native English working also in the area, we have included for each part at section 3 a last paragraph with the most significant results as indicated. Figures have been improved with all details indicated by the reviewers. The bibliography has been checked.

## ***Interactive comment on “Changes in the partial pressure of carbon dioxide in the Mauritanian-Cape Verde upwelling region between 2005 and 2012” by Melchor González-Dávila et al.***

**Anonymous Referee #1**

Received and published: 6 April 2017

Overall evaluation: The authors present many years of Carbon-VOS data from an important upwelling region of the Atlantic. They consider changes in the upwelling index in the surface waters along the route and consequent changes in carbon uptake (and changes in pH). They make some important observations of a decrease in SST and trends in seawater fCO<sub>2</sub> that can only be explained by an increased upwelling. They consider both inter-annual variability (and the influence of the NAO) and spatial (latitudinal) variability in the data.

Specific Comments: The figures are clear although I would suggest some minor changes to improve on this. For example in discussion of **Figure 2** there is reference to the months (eg: March to September) which cannot really be distinguished in the

[Printer-friendly version](#)

[Discussion paper](#)

figure (that only shows a tick mark for January). This could be improved. **Figure 3** is missing the Y-axis label (the X-axis label could also be improved by moving the units into the legend and keeping the x-axis label as 'change per year' for example). The legend should also specify the years shown. In **Figure 4** the colours used are not explained in the legend (the shift in season discussed is reliant on knowing what the colours represent). There is a clear typo in the legend suggesting 'pannels' rather than 'panels'. Figure 5 shows normalised fCO<sub>2</sub> which I hadn't seen in the method section. The legends in Figure 4 and 5 refer to 'Experimental' series rather than 'in situ' data which may be a person preference but I think 'experimental' is misleading. Figure 7 is in mmol m<sup>-3</sup> unit when the text discusses mol m<sup>-3</sup>.

The figures were changed according with the reviewer's comments. Typos, explanation about normalised data and other definitions were considered.

The text is generally well written and I would suggest that just a few inconsistencies are addressed. For example in the Abstract line 28 refers to an increase in outgassing then in line 30 the authors refer to 'this increase in CO<sub>2</sub> intake'. Throughout there is reference to 'opportunity ships', which are more easily recognised to the community as Ships of opportunity (or Carbon-VOS). When fCO<sub>2</sub> first appears (line 91) it is referred to as partial pressure rather than fugacity. The oxygen optode is mentioned on line 123 but the location of this sensor is not indicated (at intake or point of CO<sub>2</sub> measurements?)

We have changed the terms to account for the real trends, VOS was considered along the text as indicated, fCO<sub>2</sub> was defined properly and the position of the optode indicated(after the seawater pump, the intake is divided in two lines, one feeding the pCO<sub>2</sub> system and the other the oxygen sensor, the fluorometer and the seabird thermosalinometer).

Line 220 suggests a shift from high to strong upwelling, that could be quantified.

The values for the upwelling indexes were included in order to show this change, following the data on Figure 2.

Line 250 suggests that SACW is nutrient rich, which needs a reference.

The reference was added.

C2

BGD

Interactive  
comment

Printer-friendly version

Discussion paper



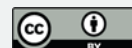
Claims in line 263 re: the position of the ITCZ in winter also require a reference  
Line 272: change arriving to arrival Line 358: Are the authors referring to annual bias or annual based (as stated)? Also change 'upwell' to 'upwelling'. Line 395: change the sentence to read that the pH rate 'is determined'.

All these technical aspects were changed as indicated.

Interactive comment on Biogeosciences Discuss., doi:10.5194/bg-2017-83, 2017.

[Printer-friendly version](#)

[Discussion paper](#)



## ***Interactive comment on “Changes in the partial pressure of carbon dioxide in the Mauritanian-Cape Verde upwelling region between 2005 and 2012” by Melchor González-Dávila et al.***

### **Anonymous Referee #2**

Received and published: 29 May 2017

Review The authors present a 7 year data record of surface ocean fCO<sub>2</sub> observations in the upwelling region off Northwest Africa. The manuscript is a solid piece of science and the data are well described. It is a very nice example how valuable data from carbon-VOS lines can be and how much we can learn from sustainable observations. The work fits perfectly in the scope of “Biogeosciences”. This said I have one major criticism: The “Results and Discussion” part is very detailed and very long, which is not bad itself. In contrast, the conclusions are very short and the main point of the paper gets a little bit diluted. The paper reads a little bit like a data paper with a lot of description and only a small part of new knowledge. One idea would be having a short summary of the major findings in each part of section 3. Then taking these summaries

[Printer-friendly version](#)

[Discussion paper](#)

and clearly highlight the major findings of this manuscript. Furthermore I suggest that the authors ask a native English speaker for proof reading.

We have followed the idea indicated by the reviewer including a short summary of the major finding in each part of section 3. The text was reviewed by a native English speaker.

Specific comments:

line 42: the authors call it here “opportunity ship” but later VOS line. I think VOS line is a commonly used term, so I suggest to introduce it here and then use it consequently in the rest of the paper.

Done

Line 58: . . . researcheRs . . .

Changed

Line 67: use “wind speed” instead of only “wind”

Done

Line 68: . . . supportS . . .

Done

Line 73/74: . . . different wind databases for the . . .

done

Line 88: . . .QUIMA-VOS line . . .

done.

Line 102: The term “VOS” is not yet introduced

This was introduced

Line 118: call is VOS line

done

BGD

Interactive  
comment

Printer-friendly version

Discussion paper



Line 125: us “. . . seawater flow but varied . . .” instead of “. . . seawater flux used but varied . . .”

done

Line 133: “. . . imposed . . .”

done

Lines 136-140: The authors report an accuracy of 1  $\mu\text{atm}$  but the standard gases don't bracket the expected  $f\text{CO}_2$  values. This is not according to SOP's and at least for the values outside the standard range the accuracy estimate should be lower.

This was improved and considered

Lines 154 ff.: To my knowledge the parameterization of Wanninkhoff (1992) has some problems and shouldn't be used. I suggest using Nightingale 2000 which has shown to produce robust flux estimates.

We agree with reviewer's comments. We have used W92 because most of the computed fluxes used that parameterization. We present the data with Nightingale parameterization.

Line 161: what does the \* mean?

This has been explained (the fitted values)

C2

Lines 166 ff: Is it proved that the general seasonal pattern follows such an sinodial approach?

We have included the errors for that fitting procedure for all variables. We have tried other functions including even the SST but there was not a significant increase in the estimation. We present the fitting between real and estimated value in order to provide the goodness of the fitting. Moreover, the data also shows how the values moves with seasons along the years. We used this model also followed by others, as Lüger et al., 2004 and in time series of data.

Lines 222 ff.: Sentence sounds odd. Please rephrase.

This was rewritten.

Line 225: The authors mention a confidence interval of  $9\text{m}^2\text{ s}^{-1}$  for the upwelling index (UI) but the scale of in Figure 3 a) is on the order of  $10\text{e-}3\text{ m}^2\text{ s}^{-1}$ . This looks like a quite large confidence interval to me.

It looks like we did not write in a clear way the values. The UI are in the order of hundreds of  $\text{m}^2\text{s}^{-1}$  and we indicated that  $\text{UI}\cdot 10^{-3}$  it is what is plotted and you have values of 0.1 to 0.3, that is until 300. A confidence interval of 9 is expected. We have wrotten this in a more readable way.

Line 240 ff.: “South of  $15^\circ\text{N}$  . . . ”; This conclusion is not clear to me. Can you please explain why a decreasing UI comes directly from an increasing SST!?

A detail explanation is included. UI were computed without temperature data. As UI decreases, less cool waters arrive to the surface: This fact together with the advection of warm water along the coast produce an increasing SST. The word “indicate” has been changed. The paragraph have been improved.

Line 265: use SST and SSS

Done

Lines 307/308: Sounds odd, please rephrase

This was rewritten

Printer-friendly version

Discussion paper





Line 312: “seasons” instead of “sea1sons”

Done

Lines 324 ff.: 4.3% would translate into an error between 15 and 26  $\mu\text{atm}$ . I think its better to give the range since the dataset includes data over a wide range.

Done

Lines 330 ff.: The word “and” in line 330 can be deleted. I don’t really understand the meaning of comparing  $\text{NfCO}_2$  (which is temp independent) with temperature again. Please explain the deeper meaning.

Done . The sentence “ $\text{NfCO}_2^{\text{sw}}$  was related with SST in order to account for effects do not removed after normalization”. This was included

Line 368: “average” instead of “averate”

Done

Line 458 ff.: sounds odd, please rephrase

Done

Line 466-469: I don’t understand the sentence. Please rephrase.

We have changed the sentence.

Line 472 ff.: The authors mention the dependence of the upwelling region on climate change forcing. Please say here clearly which forcing you mean and what the exact effect is.

This was rewritten, and the processes were indicated in the introduction part.

Line 484: Use “VOS line”

Done

Figure 2:

- please say if red or blue denotes upwelling events. It is somehow clear but this information would improve the readability.

- Done

Figure 3:

- are the units correct (see also comment above regarding the confidence interval)
- please add Latitude in °N to the y-axis
- line 228 and 229: “panel” instead of “pannel”
- the authors use “year-1” and “/year” in the same figure. Please use it consistent.

Figure 3 (now 4) was improved including those aspects (also that indicated by reviewer 1)

- Figure 4:
- Can you name the month that you used for summer, fall, winter and spring?

Done

- Figure 5:

- Instead of showing  $f\text{CO}_2$  (measured) and  $Nf\text{CO}_2$  I would suggest just showing the difference ( $Nf\text{CO}_2 - f\text{CO}_2$  (Measured)). Then there is no need to compare panel by panel, instead the deviations would be clearly visible.

We have kept  $f\text{CO}_2$  (measured) because it will be important to improve the readability. We have included the difference as indicated to see deviations.

Figure 7:

- Can you name the month that you used for summer, fall, winter and spring?

Done

Printer-friendly version

Discussion paper



C4

C3

1 **Changes in the partial pressure of carbon dioxide in the Mauritanian-Cape Verde**  
2 **upwelling region between 2005 and 2012.**

3  
4 **By**

5  
6 **Melchor González-Dávila<sup>1\*</sup>, J. Magdalena Santana Casiano<sup>1</sup> and Francisco**  
7 **Machín<sup>1,2</sup>**

8 **<sup>1</sup>Instituto de Oceanografía y Cambio Global, Grupo QUIMA, Universidad de Las**  
9 **Palmas de Gran Canaria, 35017, Las Palmas de Gran Canaria. Spain.**

10 **<sup>2</sup>Departamento de Física, Universidad de Las Palmas de Gran Canaria, 35017, Las**  
11 **Palmas de Gran Canaria**

12

13

14 \* Correspondence to [melchor.gonzalez@ulpgc.es](mailto:melchor.gonzalez@ulpgc.es)

15

16

Código de campo cambiado

17 **ABSTRACT**

18 Coastal upwelling along the eastern margins of major ocean basins represent regions of  
19 ~~large economic~~ great ecological and economic importance due to the high biological  
20 productivity. The role of these regions in the global carbon cycle makes them essential in  
21 addressing climate change. ~~However,~~ The physical forcing of upwelling processes that  
22 favor the production in these areas are already being affected by global warming, which  
23 will modify the intensity of the upwelling and, consequently, the carbon dioxide cycle.  
24 ~~For this reason, the role of observations in addressing any climate change impacts on the~~  
25 ~~global carbon cycle in areas of upwelling is of great importance.~~ Here, we present  
26 ~~Monthly~~ monthly high resolution surface experimental data for temperature and partial  
27 pressure of carbon dioxide in one of the four most important upwelling regions of the  
28 planet, the Mauritanian-Cape Verde upwelling region, from 2005 to 2012 ~~are shown~~. This  
29 data set provides direct evidence of seasonal and interannual changes in the physical and  
30 biochemical processes. Specifically, we show ~~They confirmed~~ an upwelling  
31 intensification and an increase of 0.6 Tg/yr in the CO<sub>2</sub> outgassing of 1 Tg a year of 0.6  
32 Tg a year in one of the four most important upwelling regions of the planet due to  
33 increased wind ~~despite increased~~ increase, even when primary productivity en seems to  
34 also be reinforced. This increase in CO<sub>2</sub> outgassing together with the observed decrease  
35 in sea surface temperature at the location of the Mauritanian Cape Blanc, 21°N, produced  
36 a pH decrease of  $-0.003 \pm 0.001$  per year.

37

38 **1. INTRODUCTION**

39  
40 The excess of CO<sub>2</sub> in the atmosphere, largely responsible ~~of for g~~ Global Climate-climate  
41 Changechange, has prompted research on the role of the oceans in the carbon cycle. ~~In~~  
42 ~~recent decades data from different oceans have been taken as thoroughly as possible, with~~  
43 ~~the~~ The aim in recent decades has been to assess how the oceans act as sources or sinks  
44 within the carbon cycle. To achieve this goal, high spatial and temporal observations  
45 representative of the distribution of CO<sub>2</sub> fluxes between the ocean and atmosphere are  
46 necessary. ~~In this regard, a~~ Automated instruments have been installed on ~~volunteer~~  
47 ~~observing ships (VOS) for sampling the oceans~~ serve to provide as much many  
48 observations throughout the global ocean as possible in addition to the ~~data is being~~  
49 collected at on scientific cruises and at long-term moorings ~~have been deployed in various~~  
50 ~~sites of the oceans~~ (i.e., Astor et al., 2005; Lüger et al., 2004, 2006; González-Dávila et  
51 al., 2005; 2009; Schuster et al., 2009; Ullman et al., 2009; Watson et al., 2009; Padín et  
52 al., 2010; Gruber et al., 2002; Dore et al., 2003; Santana-Casiano et al., 2007; Bates et al.,  
53 2014).

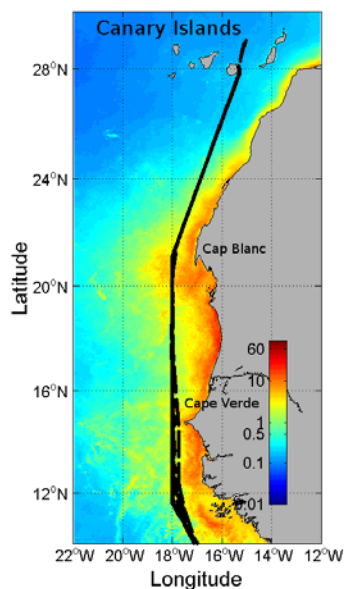
54 With the amount of data already gathered (<http://www.socat.info/>), climatologies that  
55 present average fluxes between the atmosphere and the ocean have been developed, ~~so~~  
56 identifying areas acting as a source or sink ~~are now identified~~ (Key et al., 2004; Takahashi  
57 et al., 2009). However, the low spatial resolution of these databases limits their  
58 applicability especially in coastal areas. ~~makes it lose relevant variability at relatively~~  
59 ~~low spatial scales. This occurs in coastal areas, specially in u~~ Upwelling regions, which  
60 are particularly under ~~not adequately~~ represented in such large databases. Upwelling zones  
61 present a dynamic process that raises nutrient and CO<sub>2</sub> rich water from relatively deep  
62 areas to the surface. ~~The, which are rich in nutrients and CO<sub>2</sub>. N~~ utrients reaching the

Código de campo cambiado

63 photic zone promote primary production, which consumes CO<sub>2</sub>. ~~This a process that~~  
64 ~~would generate~~s a CO<sub>2</sub> flux into the ocean (sink). On the other hand, the upwelling also  
65 brings up CO<sub>2</sub> from deep seawater, ~~which finally this~~ generates uncertainty about the  
66 actual role of upwelling areas as a source or sink of CO<sub>2</sub> (Michaels *et al.*, 2001). Indeed,  
67 ~~previous researchers indicate that~~ upwelling areas may act as a source or sink of CO<sub>2</sub>  
68 depending on their location (Cai *et al.*, 2006; Chen *et al.*, 2013), where as upwelling ~~areas~~  
69 regions at low latitudes mainly act as a source of CO<sub>2</sub> (Feely *et al.*, 2002; Astor *et al.*,  
70 2005; Friederich *et al.*, 2008; Santana-Casiano *et al.*, 2009; González-Dávila *et al.*, 2009)  
71 and those at mid-latitudes mainly act as a sink of CO<sub>2</sub> (Frankignoulle and Borges, 2001;  
72 Hales *et al.*, 2005; Borges *et al.*, 2002; 2005; Santana-Casiano *et al.*, 2009; González-  
73 Dávila *et al.*, 2009). Several anthropogenic ~~interactive~~ effects are strongly influenceing  
74 ~~the general picture for the most representative~~ Eastern Boundary Upwelling Systems  
75 (EBUS), ~~and~~ including upper ocean warming, ocean acidification, and ocean  
76 deoxygenation (Gruber, 2011; Feely *et al.*, 2008; Keeling *et al.*, 2010). Moreover,  
77 evidence ~~for an of~~ increased in wind speed that would favor upwelling (Bakun, 1990;  
78 Demarcq, 2009; Oerder *et al.* 2015) supports the possibility of a change in the dynamics  
79 ~~current role~~ of these highly productive areas. Recently, eddy-resolving regional ocean  
80 models have shown how upwelling intensification can be followed by cause a major  
81 impact on the system's biological productivity and ~~in the~~ CO<sub>2</sub> outgassing (Lachkar and  
82 Gruber, 2013; Oerder *et al.*, 2015).

83 Wind observations and reanalysis products are controversial regarding the Bakun  
84 intensification hypothesis (Bakun 1990). Using different wind databases for the Canary  
85 region, Barton *et al.* (2013) concluded that there was no evidence for a general increase  
86 in the upwelling intensity off northwest Africa while ~~Marcello~~ *et al.* (2011) found an  
87 intensification of the upwelling system in the same area during a 20-year period while the

88 alongshore wind stress remained almost stable. Cropper et al. (2014) found that coastal  
89 summer wind speed increased, resulting in an increase in upwelling-favorable wind  
90 speeds north of 20°N and an increase in downwelling-favorable winds south of 20°N.  
91 Santos et al (2005; 2012) showed ~~differences in~~ Sea Surface ~~surface~~  
92 ~~Temperature~~ temperature (-SST)  ~~were not homogeneous either along latitude or~~  
93 ~~longitude and between coast and ocean~~  depended ~~ing~~ on the upwelling index and UI  
94 ~~intensity~~ y, ~~and that SST trends were not homogeneous either along latitude or longitude.~~  
95 Varela et al. (2015) ~~also showed~~ demonstrated opposite results world-wide ~~when different~~  
96 ~~wind databases were used and when the same wind database was considered~~ depending  
97 on the length of data, season evaluated, and selected area within the same wind dataset or  
98 between datasets. For the Mauritanian region, when wind stress data were used (Varela  
99 et al., 2015), a more persistent increasing trend in upwelling-favourable winds north of  
100 21°N and a decreasing trend south of 19°N ~~were~~ was determined.  
101 Starting in June 2005, the QUIMA-VOS line visited the Mauritanian-Cape Verde  
102 upwelling region northwest of Africa on a monthly basis (Fig. 1 and Supplementary Table





103 S1) producing for the first time a high resolution [database of SST](#) and [partial pressure of](#)  
104 [CO<sub>2</sub> expressed as fugacity /CO<sub>2</sub> database](#). This database ~~has been considered to show~~s the  
105 variations in the CO<sub>2</sub> system under changes in the upwelling conditions in the Canary  
106 Ecosystem from 27°N to 10°N for the period 2005 to 2012.

107 Fig. 1. Ship track in the area from 28°N (Gran Canaria, The Canary Islands) to 10°N (black dots).  
108 The locations of Cap Blanc and Cape Verde are indicated. Monthly Ocean Color  
109 (oceancolor.gsfc.nasa.gov) data for average chlorophyll *a* concentration (mg m<sup>-3</sup>) were included  
110 in a Matlab™ routine and annually averaged ~~ed~~, ~~in order to draw the map for the area~~. The map  
111 has been generated using Matlab 7.12 R2011a.

112

## 113 2. EXPERIMENTAL

### 114 2.1 [Study Region](#) ~~evaluated~~.

115 The [VOS line crosses](#) the East Atlantic Ocean from the north of Europe (English Channel)  
116 to South Africa, calling [at](#) Gran Canaria, the Canary Islands, with a periodicity of two  
117 months, which provides monthly data (southward or northward sections). In this work,  
118 the area between Gran Canaria at 27°N and 10 °N has been selected in order to study the  
119 Mauritanian-Cape Verde upwelling region. In its ~~south~~ route [south](#) (Fig. 1), the ship  
120 leaves Gran Canaria, and goes straight to 100 ~~k~~[km](#) off Cap Blanc, at 21°N 17°45'W. It  
121 then follows this longitude, passing at 100 km off Cape Verde until 12°N, where it  
122 changes direction to Cape Town, reaching 10°N 17°W at 330 km out of the coast of  
123 Guinea. Between 22°N and 20°N, the ship reaches the 500 m isobath. South of 15°N, the  
124 ship moves between 1000 and 500 m isobath. In its ~~north~~ route [north](#), the ship follows the  
125 same reverse track.

### 126 2.2 Experimental data

127 Experimental data were obtained under the EU projects Carboocean and Carbochange  
128 ([www.CarboOcean.org](#), [https://carbochange.b.uib.no/](#)) and now also available at  
129 [http://www.socat.info/](#). An autonomous instrument for the determination of the partial  
130 pressure of CO<sub>2</sub> developed by Craig Neill following NOAA recommendations was

Código de campo cambiado

Código de campo cambiado

Código de campo cambiado

131 installed in a VOS line. This was operated by the MSC company ~~during the~~from 2005 to  
132 2008 ~~period~~ and the Maersk Company from 2010 to 2012 along the so called QUIMA-  
133 VOS line between the UK and Cape Town, from July 2005 to January 2013  
134 (Supplementary Table S1). Temperature was measured at three locations along the  
135 sampling circuit: in the intake (SeaBird SBE38L), in the equilibrator (SeaBird  
136 thermosalinograph SBE21 and internal PT100 thermometer), and in the oxygen sensor  
137 (Optode 3835 Aanderaa<sup>TM</sup>). After the seawater pump, the intake is divided in two lines,  
138 one feeding the CO<sub>2</sub> system and the other the oxygen sensor, the fluorometer and the  
139 seabird thermosalinometer. Differences between equilibrator and intake were constant in  
140 time due to the high seawater flow but varied among ships due to the different locations  
141 of the equipment. Values varied between 0.06°C when the equipment was placed close to  
142 the intake to 0.35°C, when the equipment was one floor above, inside the engine room.  
143 The SST was also obtained from the NOAA\_OI\_SST-V2 data provided by the  
144 NOAA/OAR/ESRL PSD, Boulder, Colorado, USA (<http://www.esrl.noaa.gov/psd>).  
145 These data had a spatial resolution of 1° latitude and 1° longitude and monthly averages  
146 were used. The correlation between our experimental SST data and satellite one was  
147 better than ± 1°C, and ~~reduced~~improved to ± 0.4°C after removing the most affected  
148 upwelling regions (19-22°N and 14-16°N), related to the high variability imposed by the  
149 upwelling.

150 The CO<sub>2</sub> molar fraction,  $x_{CO_2}$ , in seawater was obtained every 150 s, while  
151 atmospheric  $x_{CO_2}$  data were ~~taken~~obtained every ~~200-180~~ min. The seawater intake was  
152 located at a 10 m depth. The system was calibrated every three hours, by measuring four  
153 different standard gases with mixing ratios in the ranges of 0.0, 250-290 ppm, 380-410  
154 ppm and 490-530 ppm of CO<sub>2</sub> in the air, provided by NOAA and traceable to the World  
155 Meteorological Organisation scale. The precision of the system is greater than 0.5  $\mu$ atm

Código de campo cambiado

156 and the accuracy estimated with respect to the standard gases is of 1  $\mu\text{atm}$  inside the  
 157 standards range. For  $x\text{CO}_2$  values higher than the highest standard (532.04 ppm), the  
 158 accuracy will be reduced, even when linearity was observed in all cases inside the  
 159 standards range. The fugacity of  $\text{CO}_2$ ,  $f\text{CO}_2$  ( $\mu\text{atm}$ ), was calculated from  $x\text{CO}_2$  after  
 160 correcting for temperature differences between intake and equilibrator, according to the  
 161 expressions for the seawater given by DOE (1994). Normalised  $f\text{CO}_2$  to the mean SST for  
 162 the area ( $T_{\text{mean}}$ ) was computed following Takahashi et al. (1993)

163

$$164 \quad (Nf\text{CO}_2) = f\text{CO}_2 \cdot \exp[0.0423(T_{\text{mean}} - \text{SST})] \quad (1)$$

165

166 In order to compute a second carbonate system variable, the surface total alkalinity  
 167 was computed from sea surface salinity ( $S_{\text{SSS}}$ ) and SST (Lee et al., 2006).  $\text{pH}_T$  at the in  
 168 situ temperature was computed from  $f\text{CO}_2$  and  $A_T$  and with average annual surface ocean  
 169 total phosphate and total silicate concentrations of 0.5 and 4.8  $\mu\text{mol kg}^{-1}$ , respectively,  
 170 from the World Ocean Atlas 2009, using the carbonic acid acidity constants by Merbach  
 171 et al (1973) refitted by Dickson and Millero (1987).

172 Air-sea  $\text{CO}_2$  fluxes,  $\text{FCO}_2$  ( $\text{mmol m}^{-2} \text{d}^{-1}$ ), were evaluated as

$$173 \quad \text{FCO}_2 = 0.24 * k * s * (f\text{CO}_2^{\text{sw}} - f\text{CO}_2^{\text{atm}}) \quad (2)$$

174 where 0.24 is the scale factor,  $k$  is the gas transfer velocity,  $s$  is the  $\text{CO}_2$  solubility,  $f\text{CO}_2^{\text{sw}}$   
 175 is the seawater fugacity of  $\text{CO}_2$  and  $f\text{CO}_2^{\text{atm}}$  is the atmospheric fugacity of  $\text{CO}_2$ . In order  
 176 to evaluate  $\Delta f\text{CO}_2$  ( $\Delta f\text{CO}_2 = f\text{CO}_2^{\text{sw}} - f\text{CO}_2^{\text{atm}}$ ),  $f\text{CO}_2^{\text{atm}}$  data were linearly interpolated to  
 177 the  $f\text{CO}_2^{\text{sw}}$  time vector. A positive value for  $\text{FCO}_2$  corresponds with a  $\text{CO}_2$  outgassing  
 178 from the ocean.  $k$  ( $\text{cm h}^{-1}$ ) was evaluated with the parametrization (Nightingale et al.,

179 2000):

$$180 \quad k = (0.222 * W^2 + 0.333 * w) * (Sc/660)^{-1/2}$$

181

$$(3)$$

182 where  $W$  is the wind speed at 10 m above the sea surface ( $\text{m s}^{-1}$ ) and  $Sc$  is the Schmidt  
183 number.

184 The variables involved in estimating  $f\text{CO}_2$  data (i.e.  $f\text{CO}_2^{\text{sw}}$ ,  $f\text{CO}_2^{\text{atm}}$ , SST and SSS)  
185 were fitted to sinusoidal expressions (Lüger et al., 2004) for a given latitude as:

$$186 \quad X(\text{lat})^* = a_0 + a_1(t - 2005) + a_2\sin(2\pi t) + a_3\cos(2\pi t) + a_4\sin(4\pi t) +$$
$$187 \quad a_5\cos(4\pi t) \quad (4)$$

188 where  $a_i$  are the fitting coefficients,  $t$  is the sampling time expressed as year fraction and  
189  $X^*$  represents any of the four fitted variables. This procedure allowed us to re-construct  
190 the series of experimental data for periods not properly sampled. The variables were  
191 decomposed into an interannual term  $X(\text{lat})_t^* = a_0 + a_1(t - 2005)$  plus a periodical  
192 term  $X(\text{lat})_p^* = a_2\sin(2\pi t) + a_3\cos(2\pi t) + a_4\sin(4\pi t) + a_5\cos(4\pi t)$ , that is,  
193  $X(\text{lat})^* = X(\text{lat})_t^* + X(\text{lat})_p^*$ . The periodical term accounts for the high frequency  
194 seasonal variability, while the interannual one marks the year-to-year trend. First,  
195 observations were grouped in a natural year for a given latitude, as if they had been taken  
196 in a single year (no correction was done for interannual variability). The mean seasonal  
197 climatology data associated with the periodic coefficients (i.e.  $a_2$ ,  $a_3$ ,  $a_4$ , and  $a_5$ )  
198 throughout the sampling period were determined. Next, the interannual coefficients  $a_1$   
199 were calculated by fitting the residuals resulting from subtracting the periodical  
200 component,  $X(\text{lat})_p^*$ , from the original variable  $X(\text{lat})$ . Fixing these five coefficients ( $a_1$ -  
201  $a_5$ ), new distributions for  $f\text{CO}_2^{\text{sw}*}$ ,  $f\text{CO}_2^{\text{atm}*}$ ,  $\text{SST}^*$  and  $\text{SSS}^*$  were constructed with a daily  
202 resolution based on the curve fits given for each variable as in Eq. (4), providing the  
203 coefficient  $a_0$ . The accuracy of this fitting procedure was checked by both computing the  
204 correlation between experimental and reconstructed values and by determining the mean  
205 residuals. The Pearson coefficients were always over 0.87 for SST (average  $0.94 \pm 0.03$ ),  
206 over 0.69 for both  $f\text{CO}_2^{\text{sw}}$ ,  $f\text{CO}_2^{\text{atm}}$  (average of  $0.79 \pm 0.07$  and  $0.82 \pm 0.04$ , respectively)

207 and over 0.67 for SSS (average  $0.79 \pm 0.07$ ). The mean residual on the determination of  
208 those four variables were  $\pm 3.7 \mu\text{atm}$ ,  $\pm 1.5 \mu\text{atm}$ ,  $\pm 0.22 \text{ }^\circ\text{C}$ , and  $\pm 0.05$  for  $f\text{CO}_2^{\text{sw}*}$ ,  
209  $f\text{CO}_2^{\text{atm}*}$ ,  $\text{SST}^*$  and  $\text{SSS}^*$ , respectively. When the monthly satellite SST values were  
210 considered, the new  $\text{SSIS}^*$  function averaged for each month produced values within  $\pm$   
211  $0.47^\circ\text{C}$ , confirming that this procedure was able to fit non-sampled periods. It was  
212 assumed that the same procedure was valid for non-sampled  $f\text{CO}_2$ . Finally, daily  $\text{FCO}_2^*$   
213 time series between  $10^\circ\text{N}$  and  $27^\circ\text{N}$  with a latitudinal resolution of  $0.5^\circ$  were calculated  
214 with a standard error of estimation of  $0.5 \text{ mmol m}^{-2} \text{ d}^{-1}$  (15% of error) that produced mean  
215 residuals (experimental  $\text{FCO}_2 - \text{FCO}_2^*$ ) of  $0.4 \text{ mmol m}^{-2} \text{ d}^{-1}$  and Pearson correlation  
216 coefficients between experimental and computed  $\text{FCO}_2^*$  of  $r > 0.6$ ,  $p < 0.01$ .

217 Chlorophyll-a was calculated from measurements made by the Moderate Resolution  
218 Imaging Spectroradiometer (MODIS) aboard NASA's Aqua satellite. We used Monthly  
219 monthly averages with spatial resolution of 9 km supplied by Ocean Color  
220 (oceancolor.gsfc.nasa.gov) ~~were used~~.

221 Wind data were downloaded from the NCEP CFSR database at  
222 <http://rda.ucar.edu/pub/cfsr.html> developed by NOAA and retrieved from the NOAA  
223 National Operational Model Archive and Distribution System and maintained by the  
224 NOAA National Climatic Data Center. The spatial resolution is approximately  $0.3^\circ \times 0.3^\circ$   
225 and the temporal resolution is 6 hours. The reference height ~~of for~~ the wind data is 10 m.

226 Rainfall data were collected by the Precipitation Radar installed on the Tropical  
227 Rainfall Measuring Mission (TRMM) satellite (<http://precip.gsfc.nasa.gov>). Monthly  
228 averages with a spatial resolution of  $0.5^\circ \times 0.5^\circ$  (product 3A12, version 07) were used  
229 (Supplementary Fig. S1) in order to explain changes in seasonal surface salinity  
230 distributions.

231

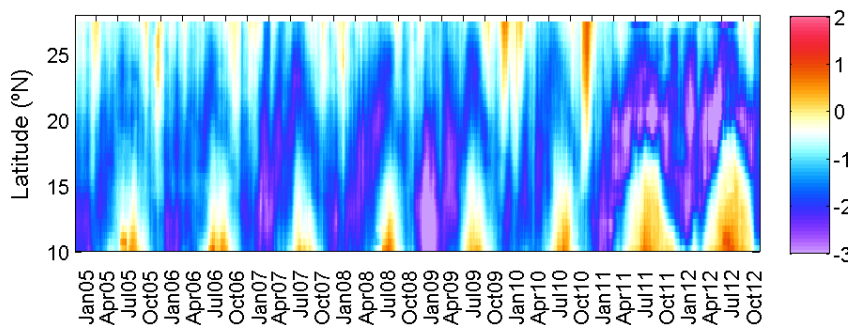
Código de campo cambiado

Código de campo cambiado

232 **3. RESULTS AND DISCUSSION**

233 **3.1 Physical properties**

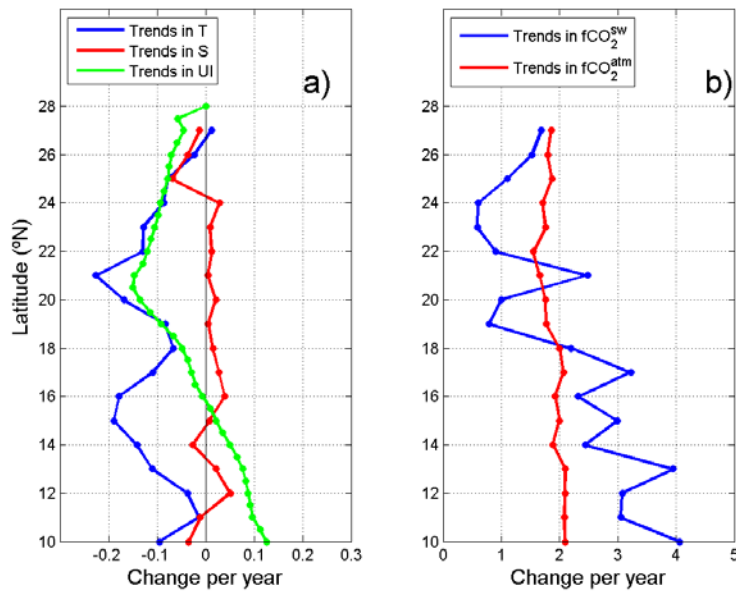
234 The variability of the Mauritanian-Cape Verde upwelling was analyzed in terms  
235 of the upwelling index (Nykjaer and Van Camp, 1994) (Fig. 2) using satellite wind data.



236  
237 Fig. 2. Time series of upwelling index ( $UI \cdot 10^{-3} \text{ m}^2 \text{ s}^{-1}$ ) in the Mauritanian-Cape Verde  
238 region along the ship track computed following Nykjaer and Van Camp (1994). Cool colours are  
239 related to upwelling events and warm colours to downwelling events.  
240

241 Negative (positive) UI values correspond to upwelling (downwelling) favorable  
242 conditions. The strongest negative values of the index correspond to more intense  
243 upwelling. Results clearly distinguish two main subareas in the upwelling system. 1)  
244 North of 20°N, the upwelling conditions were favorable throughout the year, although the  
245 highest upwellings were observed from March to September with a northward shift from  
246 20° to 22°N. 2) South of 20°N, a marked seasonality was observed with favorable. ~~South~~  
247 ~~of 15°N, in the Cape Verde area,~~ upwelling conditions were favorable during autumn and  
248 winter, with the maximum intensity observed during January and February. In this region,  
249 a downwelling regime is present between May and November when the summer. ~~At~~  
250 ~~this time, a replacement of the~~ trade winds during the summer are replaced by the  
251 monsoon al winds, ~~also~~ advecting warm water northward along the shore (Nykjaer and  
252 Van Camp, 1994). Our results (Fig. 2) are quite consistent with previous research

253 (Nykjaer and Van Camp, 1994; Marcello et al., 2011; Santos et al., 2005; 2012; Cropper  
 254 et al., 2014) but include the years 2010 to 2012 where UI at around 20-21°N presented a  
 255 shift of the upwelling regime intensity from high (-2000 m<sup>2</sup> s<sup>-1</sup>) to strong (-2800 m<sup>2</sup> s<sup>-1</sup>).  
 256 The analysis of upwelling trends along this area has been controversial since it is highly  
 257 dependent on the selected region (Santos et al., 2012). The inter-annual evolution of UI  
 258 over the period 2005 to 2012 (Fig. 3, green line) for each degree in latitude indicates an  
 259 increase in the UI (mean confidence interval of 9 m<sup>2</sup> s<sup>-1</sup>) followed that as showed by Santos  
 260 et al. (2012), indicating an increase in the UI (mean confidence interval of 9 m<sup>2</sup> s<sup>-1</sup>).



261  
 262 Fig. 34. Latitudinal distribution of the interannual trends for the Upwelling Index (UI\*10<sup>-3</sup>) and  
 263 for the four experimental variables along the QUIMA-VOS line integrated over every degree  
 264 between 2005 and 2012. The a) panel presents the trends for Upwelling index (UI\*10<sup>-3</sup> m<sup>2</sup> s<sup>-1</sup>,  
 265 mean confidence interval of 9 m<sup>2</sup> s<sup>-1</sup>), SST (°C yr<sup>-1</sup>, confidence interval 0.13°C) and SSS (yr<sup>-1</sup>,  
 266 confidence interval 0.06) and the b) panel the trends for fCO<sub>2</sub><sup>sw</sup> and fCO<sub>2</sub><sup>atm</sup> (confidence intervals  
 267 4.23 μatm and 0.44 μatm).  
 268

269 North of 15°N, the upwelling index ~~(except for the area south of 15°N where~~  
270 ~~downwelling is shown)~~ confirmed the stronger upwelling observed since 1995-1996 in  
271 this region after a more than a 10-year (from at least 1982 to 1995) period of weaker  
272 upwelling (Santos et al., 2012). Local zonal differences between ocean and coastal SST  
273 trends determined ~~by using~~with satellite data confirmed the intensification of the  
274 upwelling regime along the African coast for the period 1982 to 2000 ~~(by Santos et al.~~  
275 ~~(2005) for the period 1982 to 2000,~~ extended by Santos et al. (2012) until 2010, and  
276 extended in this study until 2012 (data not shown). ~~confirmed the intensification of the~~  
277 ~~upwelling regime along the African coast.~~ This has been described as a decadal scale shift  
278 of the upwelling regime intensity (Marcello et al., 2011; Santos et al., 2012).

279 South of 15°N, the annual UI values and trends (Fig. 2 and 3) both for the  
280 upwelling (values close to  $-2800 \text{ m}^2 \text{ s}^{-1}$  in January) and downwelling (values reaching  
281  $1850 \text{ m}^2 \text{ s}^{-1}$  in July) periods are becoming stronger. ~~At 11-12°N, were downwelling is~~  
282 becoming stronger this results resulting, however, in negative annual temperature rates  
283 that approaches to zero ~~at 11-12°N, were downwelling is becoming stronger~~. They serve  
284 as an indication of decadal variability of the summer monsoon winds and associated  
285 northward advection of warm water along the coast (Santos et al., 2012).

286 The highest upwelling intensity along the VOS line was located at the capes, Cap  
287 Blanc and Cape Verde. From satellite chlorophyll-*a* data, especially off Cap Blanc, giant  
288 filaments with chlorophyll concentrations above  $1 \text{ mg m}^{-3}$  persist year-round, spreading  
289 from the coast several hundred kilometers offshore (Fig. 1). North of Cap Blanc the  
290 upwelled water originates from the North Atlantic Central Water, and mixes with South  
291 Atlantic Central Water, SACW, towards the south (Mittelstaedt, 1983). South of Cap  
292 Blanc, the upwelling of nutrient rich SACW (Mittelstaedt, 1983) promotes phytoplankton  
293 growth between Cap Blanc and Cape Verde. Towards 12°N, upwelling is also fed by the



294 North Equatorial Under Current (Hagen and Schemainda, 1984). Moreover, the entire  
295 northwest African coast is also influenced by the African desert dust transport by the mid-  
296 tropospheric Harmattan winds originating from the central Sahara, which supplements  
297 the levels of micronutrients (such as iron) to the adjacent marine ecosystem (Mittelstaedt,  
298 1983; Neuer et al., 2004; ~~Swap et al., 1996~~).

Código de campo cambiado

Código de campo cambiado

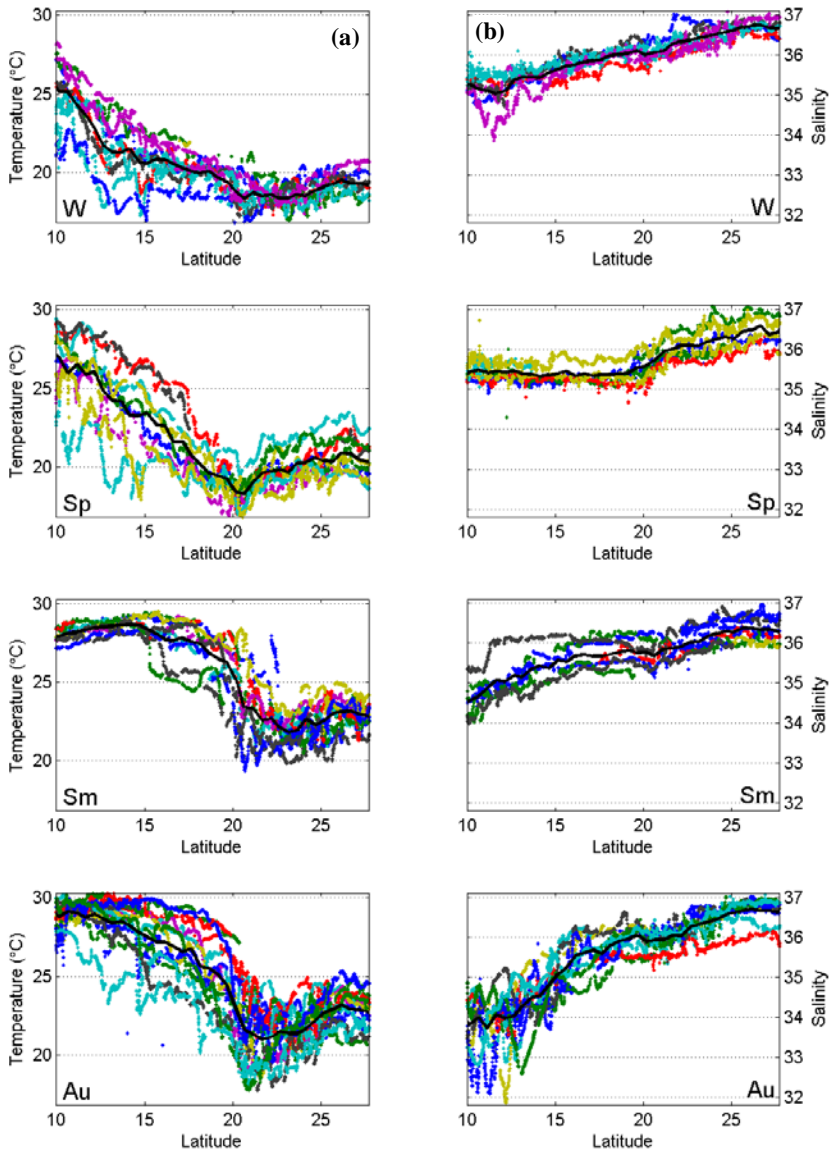
299 The area is also affected by the migration of the Inter-Tropical Convergence Zone  
300 (ITCZ), related to maximum precipitation rates (Hastenrath, 1995). To have a significant  
301 satellite precipitation record in our region of interest, precipitation data were integrated  
302 longitudinally between 25.25°W and 9.75°W. Time series for the latitudinal distribution  
303 of integrated precipitation (Supplementary Fig. S1) identified the average position of the  
304 ITCZ related to maximum precipitation rates. The ITCZ was located at its southernmost  
305 position (2°N) during winter, reaching its northernmost position (14-16°N) around  
306 summer. The ITCZ reached our area of interest (>10°N) from late spring to late summer.

307 The latitudinal distributions of measured SST and SSS along the vessel track are  
308 shown in Fig. 4, grouped by ~~seasons~~. ~~In situ temperature at 27°N shows temperatures in~~  
309 ~~the range of 18 to 24°C with the minimum in winter and maximum in late summer early~~  
310 ~~autumn. The annual temperature range was somewhat higher at 20°N, with summer~~  
311 ~~maximum of around 26°C and minimum in spring of about 17°C. At 10°N, temperatures~~  
312 ~~were the highest throughout the year (>25°C), with minimum values in winter and~~  
313 ~~maximum in late spring and late autumn. The low values observed during the end of~~  
314 ~~summer are related to the arrival of the ITZC (Supplementary Fig. S1) at those latitudes.~~  
315 ~~The thermal distribution shows a temperature increase as we move to the Equator and a~~  
316 ~~notable cooling at the upwelled waters off Mauritania.~~ The temperature generally  
317 decreased from 10°N to about 20°N to 21°N, where the ship meets the Mauritanian  
318 upwelling. From there to the north, the temperature rises as the ship leaves the upwelling

319 area on its way to the Canary Islands. [In situ temperature at 27°N shows temperatures in](#)  
320 [the range of 18 to 24°C with the minimum in winter and maximum in late summer-early](#)  
321 [autumn. The annual temperature range was somewhat higher at 20°N, with summer](#)  
322 [maximum of around 26°C and minimum in spring of about 17°C. At 10°N, temperatures](#)  
323 [were the high throughout the year \(>25°C\), with minimum values in winter and maximum](#)  
324 [in late spring and late autumn. The low values observed during the end of summer are](#)  
325 [related to the arrival of the ITCZ \(Supplementary Fig. S1\) at those latitudes. The thermal](#)  
326 [distribution shows a temperature increase as we move to the Equator and a notable](#)  
327 [cooling at the upwelled waters off Mauritania.](#) Only during winter time and the beginning  
328 of the spring, the upwelling of cold water from Cape Verde area was detected. Salinity  
329 minimum values were normally located at 10°N, increasing to maximum values at the  
330 Canaries' latitude. The minimum values of salinity were exceptionally low during autumn  
331 from 10°N to 16°N by both the freshwater input from rivers that increase their outflow  
332 during this [season](#) (Nicholson, 1981) and by the northward shift of the ITCZ during this  
333 part of the year.

334

335



336 Fig. 4. *In situ* data of a) SST and b) SSS data in the Mauritanian - Cape Verde coastal region  
 337 grouped by seasons: winter (W, December, January and February), spring (Sp, March, April and  
 338 May), summer (Sm, June, July and August) and autumn (Au, September, October and November).  
 339 The averaged values for all cruises in Table S1, are shown in black for each season including the  
 340 95% confidence limits. Colour code for each cruise is that indicated in Table S1.

341  
 342

343 Anomaly fields for temperature and salinity (data not shown) were calculated as  
344 the difference between the observations and the mean values at each season for individual  
345 latitudes. For temperature, the largest anomalies in winter and spring were located south  
346 of 18°N, with values of  $\pm 2^{\circ}\text{C}$ , related to the seasonal cycle of the Cape Verde upwelling.  
347 During summer the pattern changed and the largest anomalies were detected in the  
348 upwelling area at 18-22°N, with values of  $\pm 5^{\circ}\text{C}$  when the upwelling index for the  
349 Mauritanian area was highest (Fig. 2). In autumn, the temperature anomalies were shifted  
350 slightly to the north, 20-24°N, with values of  $\pm 3^{\circ}\text{C}$  related to the observed pulses in  
351 upwelling favorable winds that affected the surface seawater properties. On the other  
352 hand, salinity anomalies showed a very homogeneous pattern in all latitudes for winter,  
353 spring and summer, with values generally within  $\pm 0.5$ . However, during autumn  
354 important anomalies south of 18°N were observed, with values in the range of  $\pm 1.5$ . In  
355 this region, the upwelling development, the river discharge and the rainy season  
356 controlled the observed distribution (Yoo and Carton, 1990).

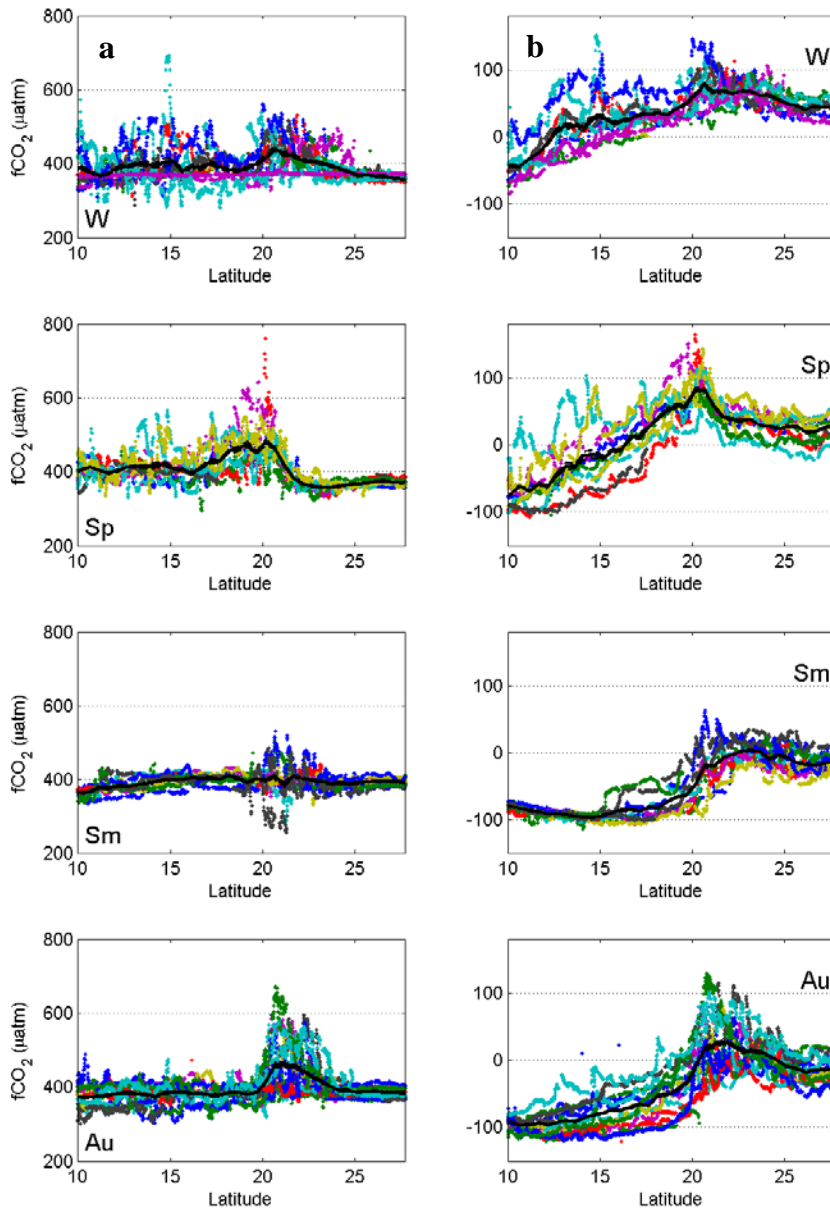
357 The data conclude a permanent annual upwelling regime observed north of 20°N  
358 and a seasonal regime across 10–19°N, in accordance with the climatology of previous  
359 studies. The data confirm also a recent increase in upwelling conditions north of 20°N  
360 and an increase in downwelling conditions south of 20°N.

361

### 362 3.2 Carbon dioxide variability

363 The latitudinal distribution of the seasonal  $f\text{CO}_2^{\text{sw}}$  data (Fig. 5a) ~~showed they were~~  
364 ~~always above the  $f\text{CO}_2^{\text{atm}}$ , with the the~~ highest values between 18 and 23°N for all seasons  
365 due to the variability imposed by the upwelling off Mauritania.  ~~$f\text{CO}_2^{\text{sw}}$  was consistently~~  
366 ~~greater than  $f\text{CO}_2^{\text{atm}}$  north of 18°N.~~ During winter, when the Cape Verde upwelling  
367 develops (Fig. 2), the 12-15°N region also presented higher  $f\text{CO}_2^{\text{sw}}$  values than those in

368 the atmosphere.  $f\text{CO}_2^{\text{sw}}$  data showed a latitudinal shift ~~along~~between the seasons  
369 following the shift observed in the upwelling index: i.e., in winter, the largest values  
370 were located between 19° and 24°N; in spring, they were located between 16° and 22°N;  
371 during summer and autumn, the largest  $f\text{CO}_2^{\text{sw}}$  values were recorded in the range 20° to  
372 23°N. The difference between  $f\text{CO}_2^{\text{sw}}$  normalized to the mean SST of 22°C for the region  
373 ( $N/f\text{CO}_2^{\text{sw}}$ ) and  $f\text{CO}_2^{\text{sw}}$  (Fig. 5b) reinforced the variability at 20-23°N all year around and  
374 at 12-17°N during winter and spring, indicating that upwelling is the major factor  
375 contributing to the  $f\text{CO}_2$  variability.  
376  
377



378

379 Fig 5. fugacity-Fugacity of CO<sub>2</sub> data in the Mauritanian-Cape Verde coastal region grouped by  
 380 seasons: winter (W), spring (Sp), summer (Sm) and autumn (Au). a)  $f\text{CO}_2^{\text{sw}}$  latitudinal  
 381 distribution. b) Difference between measured and Normalized  $f\text{CO}_2^{\text{sw}}$  values to a constant  
 382 temperature of 22°C. The averaged values for all cruises in Table S1, are shown in black for each

383 season including the 95% confidence limits. Colour code for each cruise is that indicated in Table  
384 S1.

385 According to Takahashi et al. (1993),  $f\text{CO}_2^{\text{sw}}$  increases with temperature at a rate  
386 ~~that is of~~  $4.3\% \mu\text{atm } ^\circ\text{C}^{-1}$  (between 15 and 26  $\mu\text{atm } ^\circ\text{C}^{-1}$  at in this area) in a  
387 thermodynamically controlled system. At  $27^\circ\text{N}$ , ~~the rate,~~ as SST increases, the rate was  
388 only of  $7.45 \mu\text{atm } ^\circ\text{C}^{-1}$  due first mainly to biological uptake and second also to the  $\text{CO}_2$   
389 outflux. At  $20^\circ\text{N}$  the rate became negative with a value of  $-10.9 \mu\text{atm } ^\circ\text{C}^{-1}$ , clearly  
390 indicating the important injection of cool and  $\text{CO}_2$  rich seawater at the upwelling area, ~~neither~~  
391 The injection is not being compensated by the solubility nor the biological carbon  
392 pumps. At  $10^\circ\text{N}$ , ~~as a result of the seasonal upwelling,~~ the rate was still negative, but ~~of~~  
393 only  $-4.3 \mu\text{atm } ^\circ\text{C}^{-1}$  as a result of the seasonal upwelling.  $N/\text{CO}_2^{\text{sw}}$  was related with SST  
394 (data not shown) in order to account for effects do not removed after during  
395 normalization. At latitudes  $19^\circ$  to  $21^\circ\text{N}$ , in the upwelling vicinity of Cap Blanc, an inverse  
396 relationship of  $70\text{-}100 \mu\text{atm } ^\circ\text{C}^{-1}$  was found during winter and spring, while in summer  
397 and autumn the inverse relationship was reduced to  $12\text{-}18 \mu\text{atm } ^\circ\text{C}^{-1}$ . While the upwelling  
398 indexes at those latitudes were quite constant throughout the year, ~~the~~ different rates  
399 observed should be related to biological consumption of the  $\text{CO}_2$  excess. However,  
400 During during winter and spring the injection of  $\text{CO}_2$  in the upwelling is not decreased by  
401 the biological activity in the area. But during the Chl-a maximum At (late the end of spring  
402 and during to summer) the Chl-a content reached its maximum and most of the  $\text{CO}_2$  was  
403 consumed and/or exported and, therefore, the rate was strongly reduced.

404 Figure 3 depicts the observed interannual trends ( $a_1$  coefficient in Eq. 4) for the  
405 four experimentally recorded detrended parameters, together with the UI trend.  
406 Confidence intervals of the computed mean annual values for SST, SSS,  $f\text{CO}_2^{\text{atm}}$ ,  $f\text{CO}_2^{\text{sw}}$   
407 were  $0.13^\circ\text{C}$ ,  $0.06$ ,  $0.44 \mu\text{atm}$  and  $4.23 \mu\text{atm}$ , respectively. There was a clear SST trend  
408 whereby seawater along the VOS line track was getting cooler with maximum cooling

409 rates at the location of Cap Blanc (21°N) and Cape Verde upwellings (15°N) with rates  
410 higher than  $-0.2^{\circ}\text{C yr}^{-1}$ . Data from the first three years (2005 to 2008) at 21°N showed  
411 lower temperatures with higher cooling rates that reached  $-0.7^{\circ}\text{C yr}^{-1}$ , although three years  
412 of data are not representative. The area crossed by the VOS line along  $17^{\circ}45' \text{W}$  from  
413  $22^{\circ}\text{N}$  to  $10^{\circ}\text{N}$  is located inside the 1000 m isobath that is well inside the mean frontal  
414 activity in the Canary region, ~~of~~ about 200 km ~~width-wide~~ (Wang et al., 2015). The  
415 different changes in temperature in the coastal slope and offshore waters are related to the  
416 different origins of the waters upwelled from depths of about 100 m to the surface  
417 (Mittelstaedt, 1983) that spread off the coastal area. The offshore water SST is less  
418 variable owing to longer residence time in the ocean surface. These effects and the fact  
419 that the VOS line keeps a track line that crossed the upwelling cells at a distance to the  
420 coast that varies among cells, contributes to the observed spatial variability. There was  
421 no attempt to compare latitudinal and longitudinal effects on the observed values. Our  
422 experimental data, however, does not show any positive SST rates in the upwelling  
423 affected area, and only when the ship approached the Canary Islands, the trends became  
424 less negative, reaching a value of  $+0.02^{\circ}\text{C yr}^{-1}$  at  $27^{\circ}\text{N}$ , similar to those obtained for  
425 oceanic Atlantic water (Bates et al., 2014).

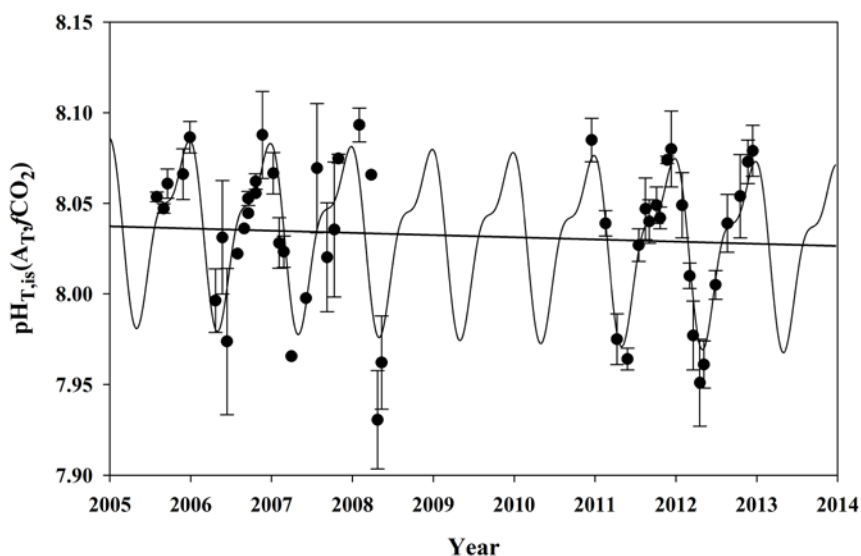
426  $f\text{CO}_2^{\text{atm}}$  for the area presented the interannual increase of about  $2 \pm 0.3 \mu\text{atm y}^{-1}$   
427 observed in atmospheric stations, while  $f\text{CO}_2^{\text{sw}}$  presented a heterogeneous distribution.  
428 South of  $18^{\circ}\text{N}$  the rate of increase was always higher than that in the atmosphere reaching  
429 a maximum value of  $4.1 \pm 0.4 \mu\text{atm y}^{-1}$  at  $10^{\circ}\text{N}$ . At  $27^{\circ}\text{N}$ ,  $f\text{CO}_2^{\text{sw}}$  increased at a rate of  
430  $1.7 \pm 0.2 \mu\text{atm y}^{-1}$  similar to that determined at the ESTOC time series site (González-  
431 Dávila et al., 2010) located at  $29^{\circ}10' \text{N } 15^{\circ}30' \text{W}$ . In the Cap Blanc area,  $f\text{CO}_2^{\text{sw}}$  increased  
432 at an average rate of  $2.5 \pm 0.4 \mu\text{atm y}^{-1}$  with the highest values in the period 2005 to 2008  
433 (a rate of  $4.6 \pm 0.5 \mu\text{atm y}^{-1}$  was computed with only those years). Around Cap Blanc,



434  $f\text{CO}_2^{\text{sw}}$  always presented lower rates of increase than in the atmosphere with values well  
435 below  $1 \mu\text{atm y}^{-1}$ . The observed decrease in SST and the trends in  $f\text{CO}_2^{\text{sw}}$  can only be  
436 explained by a reinforced upwelling. North of  $18^\circ\text{N}$ , the lowest rate of increase in  $f\text{CO}_2^{\text{sw}}$   
437 compared to  $f\text{CO}_2^{\text{atm}}$ , together with a decrease in temperature, indicated that upwelling is  
438 also favoring an increase in the net community production around the Mauritanian  
439 upwelling, consuming and/or exporting the  $\text{CO}_2$  rich upwelled waters favored by the  
440 lateral transport of the Mauritanian current (Lachkar and Gruber, 2013; Varela et al.,  
441 2015). The upwelling intensification effects observed in the trends of our experimental  
442 data support the recent wind stress trends (Crooper et al., 2014; Varela et al., 2015; Santos  
443 et al., 2012) of increased upwelling-favorable winds, at least for the period 2005-2012 in  
444 the Canary upwelling region (Fig. 2 and 3). The intensification of the upwelling results  
445 in a change in the measured upwelled water properties due to either higher upwelling  
446 velocities or deeper source upwelled waters. However, what remains unclear from these  
447 records is to what extent those changes reflect upwelling variations due to climate change  
448 forcing versus natural decadal variability in the upwelling areas occurring over  
449 interannual timescales.

450 Because ~~of~~ the upwelling intensity is changing, other variables will also be  
451 affected.  $\text{pH}_{\text{T, is}}$  at  $21 \pm 0.25^\circ\text{N}$  was computed from  $f\text{CO}_2$  and alkalinity pairs of data.  
452 Alkalinity was computed from regional correlations with SST and SSS (Lee et al., 2006)  
453 which could under-represent seasonal and interannual variations in upwelling areas.  
454 However, pH computed from  $f\text{CO}_2$  values are relatively insensitive to errors in  $A_{\text{T}}$ , and  
455  $f\text{CO}_2$  controls the magnitude and variability of pH (a  $60 \mu\text{mol kg}^{-1}$  change in  $A_{\text{T}}$  will affect  
456 a 0.1% in pH, that is, about 0.01 pH units). Figure 6 depicts the computed  $\text{pH}_{\text{T, is}}(A_{\text{T}},$   
457  $f\text{CO}_2)$  data and the harmonic fitting Eq. (4) providing seasonal variability and interannual  
458 trend. Considering the small systematic biases in interannual dynamics, ~~it is we~~

459 determined a decrease in pH at a rate of  $-0.003 \pm 0.001$  per year (Fig. 6). This decrease is  
 460 one of the highest rate values determined in several time series stations (Bates et al.,  
 461 2014), where oceanic SST has only slightly increased in the last decades. However, at the  
 462 Mauritanian upwelling area and at the location where our VOS line approached this  
 463 region, SST decreased at a rate of  $-0.22 \pm 0.06^\circ\text{C y}^{-1}$  (Fig. 3). Solely, this decrease in  
 464 temperature would increase the pH by a rate of  $+0.004 \text{ yr}^{-1}$  and the  $f\text{CO}_2$  would decrease  
 465 by  $4 \mu\text{atm yr}^{-1}$ . The net effect of the increase in the amount of rich  $\text{CO}_2$ /low pH upwelled  
 466 waters in the Mauritanian upwelling would be, therefore, a decrease in the pH of over -  
 467  $0.007 \pm 0.002$  units  $\text{y}^{-1}$  and an increase in  $f\text{CO}_2$  of  $+6.5 \pm 0.7 \mu\text{atm y}^{-1}$  (with periods where  
 468 those rates could reach values of  $0.015 \text{ y}^{-1}$  in pH and  $10.5 \mu\text{atm y}^{-1}$  in  $f\text{CO}_2$  as recorded  
 469 during 2005-2008). Those values are greatly compensated by the important decrease in



470 the SST resulting in the determined rates of  $-0.003 \pm 0.001$  pH units and  $+2.5 \pm 0.4$   
 471  $\mu\text{atm of } f\text{CO}_2$  per year.

472 Fig. 6. pH at *in situ* SST in total proton scale computed from total alkalinity (based on regional  
 473 correlations with SST and SSS, Lee et al., 2006) and  $f\text{CO}_2$  at  $21 \pm 0.25^\circ\text{N}$ . The error bar represents  
 474 the standard deviation of the computed data for each cruise for the selected latitude. The black  
 475 line shows the harmonic fitting Eq. (4) for the data and the corresponding linear trend.

476

477 This new data set of experimental values confirmed a decrease in SST and trends in  
478  $f\text{CO}_2^{\text{sw}}$  than can only be explained by a-reinforced upwelling conditions, that favor an  
479 increase in the net community production around the Mauritanian upwelling together with  
480 a more corrosive environment with pH values that decrease by over  $-0.007 \pm 0.002$  units  
481 at  $21^\circ\text{N}$ . However, the decrease in SST in the upwelling cell buffers this rate to values  
482 around  $-0.003 \pm 0.001$  pH units  $\text{yr}^{-1}$  and  $+2.5 \pm 0.4$   $\mu\text{atm yr}^{-1}$  in  $f\text{CO}_2$ , in the highest range  
483 for other time series studies.

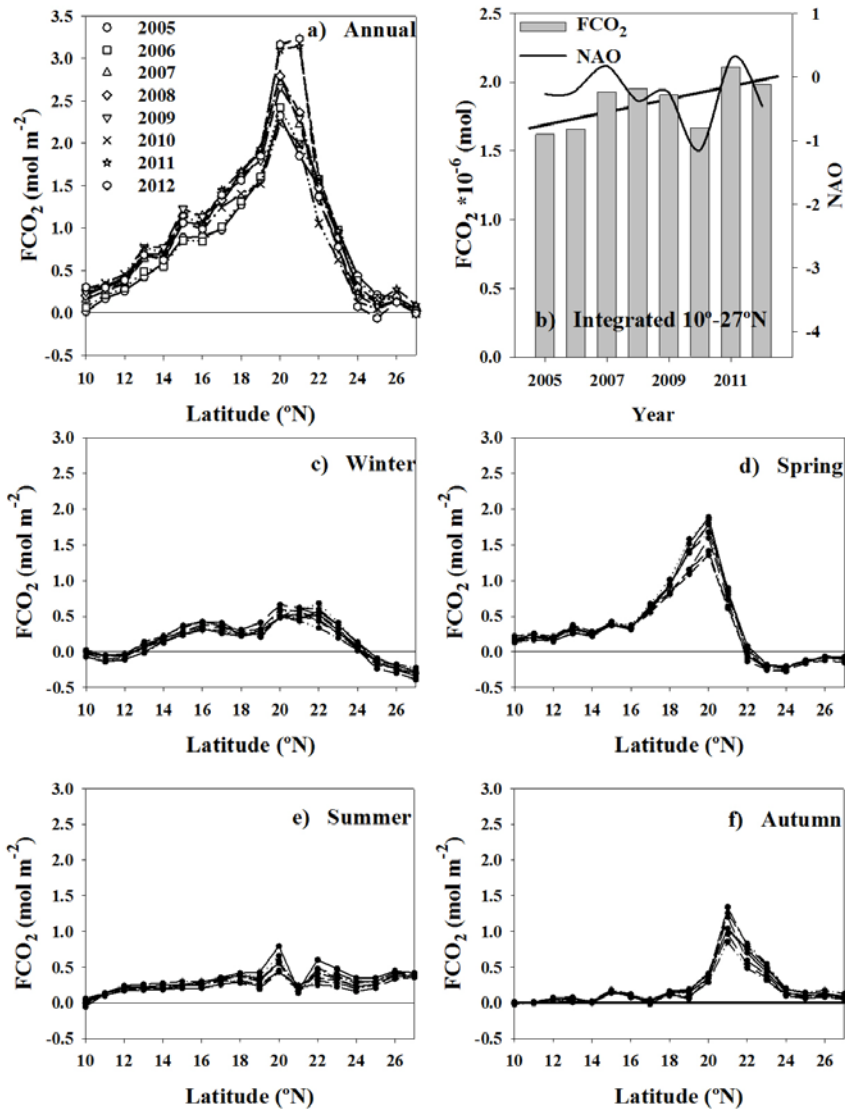
484

### 485 **3.3 Fluxes of CO<sub>2</sub>**

486 The annual air-sea CO<sub>2</sub> flux for the full domain was positive (Fig. 7a), with the area off  
487 Mauritania, between 18 and 22°N, acting as an active source of CO<sub>2</sub> to the atmosphere

488

489



490  
 491 Fig. 7. Latitudinal distribution of seasonal and annual CO<sub>2</sub> fluxes, FCO<sub>2</sub> (mol m<sup>-2</sup>). Fluxes of CO<sub>2</sub>  
 492 were computed using Nightingale et al. (2000) parametrization and satellite winds with a  
 493 resolution of 6 hours. a) Integrated year-to-year from 2005 to 2012 and b) latitudinally integrated  
 494 for 2005 to 2012 together with annual values for NAO index. Latitudinal distribution of FCO<sub>2</sub>  
 495 seasonally integrated from 2005 to 2012 are depicted for winter (c, December, January and  
 496 February), spring (d, March, April and May), summer (e, June, July and August) and autumn (f,  
 497 September, October and November).

498

499 with values close to  $3.3 \text{ mol CO}_2 \text{ m}^{-2}$  (Fig. 7a). North of  $24^\circ\text{N}$ , in the area not affected by  
500 the coastal upwelling, an average flux of  $+0.14 \pm 0.03 \text{ mol CO}_2 \text{ m}^{-2}$  was determined.  
501 The ingassing observed during winter and spring of  $-0.165 \pm 0.0327 \text{ mmol CO}_2 \text{ m}^{-2}$  for  
502 the full period (Fig. 7) was surpassed by the outgassing during summer and autumn of  
503  $0.28285 \pm 0.14140 \text{ mmol CO}_2 \text{ m}^{-2}$ . South of  $24^\circ\text{N}$ , it was observed that during spring (Fig.  
504 7d) the photosynthetic activity was not intense enough to uptake the  $\text{CO}_2$  injected by the  
505 strongest upwelling in the surface waters and thus the area acted as a source of  $\text{CO}_2$  with  
506 values reaching  $1.9 \text{ mol CO}_2 \text{ m}^{-2}$  in 2012. During summer (Fig. 7e), primary producers  
507 and lateral advection of warm waters by the Mauritanian current could consume/export  
508 the  $\text{CO}_2$  rich waters reaching values of  $0.5 \text{ mol m}^{-2}$ . During autumn (Fig. 7f), only the area  
509 between  $20^\circ\text{N}$  and  $23^\circ\text{N}$  acted as a source of  $1-1.5 \text{ mol CO}_2 \text{ m}^{-2}$ , while the rest was almost  
510 in equilibrium. ~~It was also detected that the late~~ autumn-winter upwelling in the  $14^\circ$   
511 to  $17^\circ\text{N}$  region contributed to an increased outgassing with a second annual submaximum  
512 of about  $0.4 \text{ mol CO}_2 \text{ m}^{-2}$  in winter (Fig. 7c). South of  $14^\circ\text{N}$ , annual  $\text{CO}_2$  fluxes decreased  
513 from about  $0.7 \text{ mol m}^{-2}$  at  $14^\circ\text{N}$  to being roughly in equilibrium at  $10^\circ\text{N}$ .

514 The integrated  $\text{CO}_2$  fluxes for the area  $10^\circ$  to  $27^\circ\text{N}$  along the VOS line section for  
515 the years 2005 to 2012 (Fig. 7b) were between  $1.6$  and  $2.1 \cdot 10^6 \text{ mol}$ , with an important  
516 ~~inter~~annual variability.  $\text{FCO}_2$  increased during the studied period by  $0.05 \pm 0.02 \cdot 10^6 \text{ mol}$   
517 ~~yr~~<sup>-1</sup>. The augment in  $\text{FCO}_2$  is related to the observed increase in wind speed (Fig. 3,  
518 indicated as UI) north of  $16^\circ\text{N}$ . ~~North of  $19^\circ\text{N}$ , the influence of the wind speed that~~  
519 far surpassed the effect of the smaller annual rate of increase in  $f\text{CO}_2^{\text{sw}}$  ~~than in relative to~~  
520  $f\text{CO}_2^{\text{atm}}$  ~~north of  $19^\circ\text{N}$  with the an~~ exception at  $21^\circ\text{N}$  (Fig. 3). South of  $16^\circ\text{N}$ , the decrease  
521 in wind speed did not exceed the effect of the incremental change in  $\Delta f\text{CO}_2$  associated ~~to~~  
522 ~~with the increased in~~ downwelling indexes (Fig. 3; Santos et al., 2012), ~~and resulting in a~~  
523 ~~slightly increasing~~  $\text{FCO}_2$  ~~was slightly ascending~~. The variability observed in the annual

524 integrated CO<sub>2</sub> fluxes (Fig. 7b) was related with the basin-scale oscillations, the North  
525 Atlantic Oscillation (NAO) index and the East-Atlantic Pattern (EA)  
526 (<http://www.cpc.ncep.noaa.gov/data/teledoc/telecontents.shtml>). Cropper et al. (2014)  
527 found winter upwelling variability was strongly correlated with the winter NAO (r values  
528 ranged from 0.50 at 12–19°N to 0.59 at 21–26°N), due to the [influence of the strength of](#)  
529 ~~the~~ Azores semi-permanent high-pressure system [on the strength of the](#), ~~which modifies~~  
530 trade wind ~~strengths~~. The annual integrated FCO<sub>2</sub> was related with the annual NAO  
531 index (Fig. 7b) with a similar r = 0.54, even when fluxes are not only controlled by wind  
532 strength. However, Fig. 7a clearly indicates that the Mauritanian upwelling area was the  
533 most important contributor to FCO<sub>2</sub> ~~in the study area. There~~ Here, the ~~FCO<sub>2</sub>~~  
534 was not ~~a~~ significantly ~~correlated~~ ~~coefficient~~ with the winter NAO (r = 0.23). Also,  
535 the EA index, ~~because which~~ represents ~~the a~~ southward-shifted NAO-like oscillation,  
536 presented a lower significant value (r = 0.48) ~~(trends not shown), as it was observed by~~  
537 ~~agreement with~~ the upwelling index (Cropper et al., 2014). ~~Overall, t~~ The correlation  
538 between fluxes and climate indexes describing the main mode of variability across the  
539 Atlantic sector may be directly related to the Azores High and its influence on the trade  
540 wind strength.

541 FCO<sub>2</sub> values along the QUIMA-VOS line were used in order to compute a flux  
542 budget for the Mauritanian-Cape Verde region. The observed values were assumed to be  
543 valid for at least 100 km to both sides of the QUIMA-VOS line. If the FCO<sub>2</sub> values are  
544 ~~assumed to be valid for at least 100 km to both sides of the QUIMA-VOS line,~~ the total  
545 flux of CO<sub>2</sub> being ejected to the atmosphere would reach a value of 16 Tg of carbon  
546 dioxide a year for the period 2005-2012, with a rate of increase of 0.6 Tg yr<sup>-1</sup>. However,  
547 it should be considered that the export of the rich fCO<sub>2</sub> upwelled water with high nutrient  
548 concentration off the coastal areas would promote a decrease in surface fCO<sub>2</sub> values (as

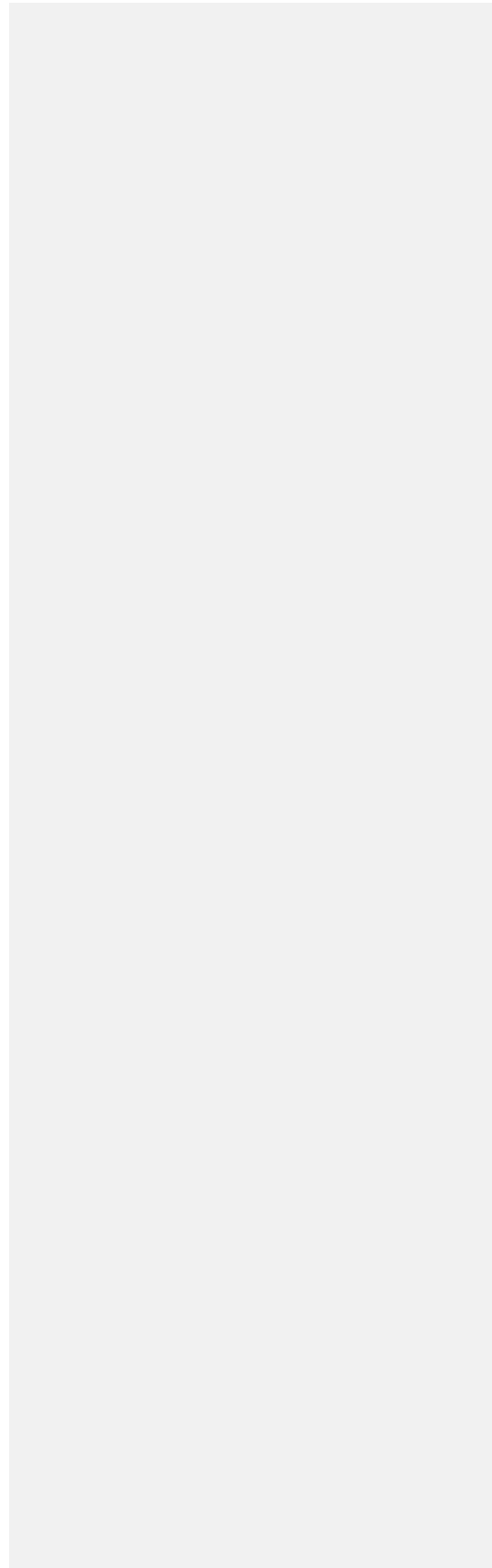
549 those observed north and south of 21°N) that will produce an ingassing of CO<sub>2</sub>. This could  
550 balance the observed outgassing increase in a more global scale.

551

#### 552 4. CONCLUSIONS

553 The Mauritanian-Cape Verde upwelling ~~area's has been shown to be an important area~~  
554 sensitive to ~~decadal and climate change~~ climatic forcing on upwelling processes, which  
555 strongly affects the CO<sub>2</sub> surface distribution, ocean acidification rates, and air-sea CO<sub>2</sub>  
556 exchange.

557 The ~~experimental SST and carbon dioxide system variable~~ results for the period 2005 to  
558 2012 confirm, ~~firstly, the~~ upwelling intensification at the Mauritanian-Cape Verde  
559 upwelling system ~~by using experimental SST and carbon dioxide system variables.~~  
560 ~~Secondly~~ Furthermore, ~~we've shown~~ that upwelling regions at low-mid latitudes are  
561 ~~strong important~~ sources of CO<sub>2</sub> to the atmosphere. ~~As a~~ and ~~thirdly, that as a direct~~  
562 result, the pH is decreasing at a rate of  $-0.003 \pm 0.001$  per year. ~~and~~ ~~Importantly,~~ the  
563 amount of emitted CO<sub>2</sub> is increasing annually at a rate of 0.6 Tg due to ~~stronger~~ wind  
564 ~~increase stress,~~ even when primary production seems to also be ~~reinforced enhanced~~ in  
565 the upwelling area. The ~~monthly record in this EBUS is not yet long enough to determine~~  
566 ~~the~~ extent to which ~~these~~ changes can be attributed to natural decadal variability ~~in this~~  
567 ~~EBUS over interannual timescales remains unclear and more years of monthly data~~  
568 ~~should be recorded.~~ ~~Sustaining~~ ~~these~~ VOS lines ~~must be maintained for years to come, and~~  
569 ~~are shown as will continue to be~~ one of the most significant contributors to ~~the our~~  
570 knowledge of how ocean surface waters are being affected by present and future climate  
571 change. The results from VOS lines can provide accurate data for changes in SST, FCO<sub>2</sub>  
572 and, consequently, upwelling intensification effects due to global change conditions  
573 under decadal natural variability.





575 **Data availability.**

576 All data are free available at the SOCAT data base, <http://www.socat.info/> and at the  
577 Carboocean and Carbochange web pages [www.CarboOcean.org](http://www.CarboOcean.org),  
578 <https://carbochange.b.uib.no/>, respectively

Código de campo cambiado

Código de campo cambiado

Código de campo cambiado

579  
580

581 **Team List**

582 Melchor Gonzalez Davila, Professor of Marine Chemistry at the University of Las Palmas  
583 de Gran Canaria. [Melchor.gonzalez@ulpgc.es](mailto:Melchor.gonzalez@ulpgc.es)

Código de campo cambiado

584 J. Magdalena Santana Casiano, Professor of Chemical Oceanography at the University of  
585 Las Palmas de Gran Canaria. [Magdalena.santana@ulpgc.es](mailto:Magdalena.santana@ulpgc.es)

Código de campo cambiado

586 Francisco Machin, Associated Professor of Physical Oceanography at the University of  
587 Las Palmas de Gran Canaria. [Francisco.machin@ulpgc.es](mailto:Francisco.machin@ulpgc.es)

Código de campo cambiado

588

589 **Author contributions**

590 M.G.D. and J.M.S.C worked in the equipment installation, data collection and designed  
591 the study. F.M. processed the data, generated figures and results. All of them collaborated  
592 in the discussion of the data and the writing of the paper.

593

594 **Competing interests**

595 There is not any competing interest.

596

597

598 **Acknowledgements**

599 Financial support from the European Union through the Integrated Project FP6  
600 CarboOcean under grant agreement no. 511106-2, FP7 project CARBOCHANGE under  
601 grant agreement no. 264879 and H2020 project ATLANTOS are gratefully

602 acknowledged. Special thanks go to the Mediterranean Shipping Company (MSC) (years  
603 2005- 2008) and the Maersk Company (years 2010-2013) who provided the ship  
604 platforms and scientific facilities. We thanks A. Abbott (Macquarie University, Sydney)  
605 for her comments and english correction. The Modis-Aqua Ocean Color Data, 2005-2012  
606 reprocessing, NASA OB.DAAC, Greenbelt, MD, USA is strongly acknowledged.

607

608 **References**

609

610 **Astor**, Y., Scranton, M., Muller-Karger, F., Bohrer, R.n and Garcia, J.: CO<sub>2</sub> variability  
611 at the CARIACO tropical coastal upwelling time series station, *Mar. Chem.*, 97(3), 245–  
612 261, 2005.

613 **Bakun**, A.: Global climate change and intensification of coastal ocean upwelling, *Science*,  
614 247(4939), 198–201, 1990.

615 **Barton**, E. D., Field, D.B., and Roy, C.: Canary current upwelling: More or less?, *Prog.*  
616 *Oceanogr.*, 116, 167-178, 2013.

617 **Bates**, N. R., Astor, Y. M., Church, M. J., Currie, K., Dore, J. E., González-Dávila, M.,  
618 Lorenzoni, L., Muller-Karger, F., Olafsson, J., and Santana-Casiano, J. M.: A time-series  
619 view of changing ocean chemistry due to ocean uptake of anthropogenic CO<sub>2</sub> and ocean  
620 acidification, *Oceanography* 27(1), 126–141, doi:10.5670/oceanog.2014.16, 2014.

621 **Borges**, A. V., and Frankignoulle, M.: Distribution of surface carbon dioxide and air-sea  
622 exchange in the upwelling system off the Galician coast, *Global Biogeochem. Cycles*,  
623 16(2), 1020, doi:10.1029/2000GB001385, 2002.

624 **Borges**, A. V., Delille, B., and Frankignoulle, M.: Budgeting sinks and sources of CO<sub>2</sub> in  
625 the coastal ocean: Diversity of ecosystems counts, *Geophys. Res. Letters*, 32, L14601,  
626 doi:10.1029/2005GL023053, 2005.

627 **Cai**, W.-J., Dai, M., Wang, Y.: Air–sea exchange of carbon dioxide in ocean margins:  
628 a province-based synthesis, *Geophys. Res. Lett.*, 33, L12603,  
629 doi:10.1029/2006GL026219, 2006.

630 **Chen**, C. T. - A., Huang, T. -H., Chen, Y. C., Bai, Y., He, X., and Kang, Y.: Air-sea  
631 exchanges of CO<sub>2</sub> in the world’s coastal seas, *Biogeosciences*, 10, 6509-6544,  
632 doi:10.5194/bg-10-6509-2013, 2013.

633 **Cropper**, T. E., Hanna, E., and Bigg, G. R.: Spatial and temporal seasonal trends in coastal  
634 upwelling off Northwest Africa, 1981–2012, *Deep-Sea Res. I*, 86, 94–111, 2014.

635 **Demarcq**, H.: Trends in primary production, sea surface temperature and wind in  
636 upwelling systems (1998–2007), *Prog. Oceanogr.*, 83, 376–385,  
637 doi:10.1016/j.pocean.2009.07.022, 2009.

638 **Dickson**, A. G., Millero, F. J.: A comparison of the equilibrium constants for the  
639 dissociation of carbonic acid in seawater media, *Deep-Sea Res.*, 34, 1733–1743, 1987.

640 DOE. Handbook of methods for the analysis of the various parameters of the carbon  
641 dioxide system in sea water, ORNL/CDIAC-74, [http://cdiac.ornl.gov/oceans/  
642 handbook.html](http://cdiac.ornl.gov/oceans/handbook.html), 1994 (date of access 07/03/2017)  
643 Dore, J. E., Lukas, R. , Sadler, D. W., and Karl, D. M.: Climate-driven changes to the  
644 atmospheric CO<sub>2</sub> sink in the subtropical North Pacific Ocean, *Nature*, 424(6950), 754–  
645 757, 2003.  
646 Feely, R. A., Boutin, J., Cosca, C. E., Dandonneau, Y., Etcheto, J., Inoue, H. Y., Ishii,  
647 M., Quéré, C. L., Mackey, D. J., McPhaden, M., Metzl, N., Poisson, A., and Wanninkhof,  
648 R.: Seasonal and interannual variability of CO<sub>2</sub> in the equatorial Pacific, *Deep Sea Res.*  
649 *II*, 49(13), 2443–2469, 2002.  
650 Feely, R.A., Sabine, C. L., Hernandez-Ayon, J.M., Ianson, D., and Hales, B.: Evidence  
651 for upwelling of corrosive ‘acidified’ water onto the continental shelf, *Science*, 320  
652 (5882), 1490–1492, doi:10.1126/science.1155676, 2008.  
653 Frankignoulle, M., and Borges, A. V.: European continental shelf as a significant sink for  
654 atmospheric carbon dioxide, *Global Biogeochem. Cycles*, 15(3), 569–576, 2001.  
655 Friederich, G. E., Ledesma, J., Ulloa, O., and Chavez, F. P.: Air-sea carbon dioxide fluxes  
656 in the coastal southeastern tropical Pacific, *Prog. Oceanogr.*, 79(2-4), 156 – 166, 2008.  
657 González Dávila, M., Santana-Casiano, M. J., Merlivat, L., Barbero-Munoz, L., and  
658 Dafner, E.: Fluxes of CO<sub>2</sub> between the atmosphere and the ocean during the POMME  
659 project in the northeast Atlantic Ocean during 2001, *J. Geophys. Res.*, 110(C7), C07S11,  
660 2005.  
661 González-Dávila, M., Santana-Casiano, J. M., and Ucha, I.: Seasonal variability of fCO<sub>2</sub>  
662 in the Angola-Benguela region, *Prog. Oceanogr.*, 83, 124–133, 2009.  
663 González-Dávila, M., Santana-Casiano, J. M., Rueda, M., and Llinás, O.: The water  
664 column distribution of carbonate system variables at the ESTOC site from 1995 to 2004,  
665 *Biogeosciences*, 7, 3067-3081, 2010.  
666 Gruber, N. Warming up, turning sour, losing breath: ocean biogeochemistry under global  
667 change, *Philos. Trans. R. Soc. London, Ser. A*, 369 (1943), 1980–1996, 2011.  
668 Gruber, N., Keeling, C. D., and Bates, N. R.: Interannual variability in the North Atlantic  
669 Ocean carbon sink, *Science*, 298(5602), 2374–2378, 2002.  
670 Hagen, E., Schemainda, R. Der Guineadom im ostatlantischen Stromsystem, *Beitr.*  
671 *Meereskd.*, 51, 5–27, 1984.  
672

673 [Hastenrath, S. Climate Dynamics of the Tropics, 488 pp., Kluwer Acad., Norwell,](#)  
674 [Mass.1995.](#)

675 [Hales, B., Takahashi, T., and Bandstra, L.:](#) Atmospheric CO<sub>2</sub> uptake by a coastal  
676 upwelling system, *Global Biogeochemical Cycles*, 19(1), GB1009, 2005.

677 [Keeling, R. F., Kortzinger, A., and Gruber, N.:](#) Ocean deoxygenation in a warming world,  
678 *Annu. Rev. Mar. Sci.*, 2, 199–229; doi:10.1146/annurev.marine.010908.163855, 2010.

679 [Key, R., Kozyr, A., Sabine, C., Lee, K., Wanninkhof, R., Bullister, J., Feely, R., Millero,](#)  
680 [F. J., Mordy, C., and Peng, T. - H.:](#) A global ocean carbon climatology: Results from  
681 GLODAP, *Global Biogeochem. Cycles*, 18, GB4031, 2004.

682 [Lachkar, Z., and Gruber, N.:](#) Response of biological production and air–sea CO<sub>2</sub> fluxes  
683 to upwelling intensification in the California and Canary Current Systems, *J. Mar. Sys.*,  
684 109–110, 149–160, 2013.

685 [Lee, K., Tong, L. T., Millero, F. J., Sabine, C. L., Dickson, A. G., Goyet, C., Park, G. H.,](#)  
686 [Wanninkhof, R., Feely, R. A., and Key, R. M.:](#) Global relationships of total alkalinity  
687 with salinity and temperature in surface waters of the world’s oceans, *Geophys. Res. Lett.*  
688 33, L19605, doi:10.1029/2006GL027207, 2006.

689 [Lüger, H., Wallace, D. W., Körtzinger, A., and Nojiri, Y.:](#) The pCO<sub>2</sub> variability in the  
690 midlatitude North Atlantic Ocean during a full annual cycle, *Global Biogeochem. Cycles*,  
691 18(3), GB3023, doi:10.1029/2003GB002200, 2004.

692 [Lüger, H., Wanninkhof, R., Wallace, D. W., and Körtzinger, A.:](#) CO<sub>2</sub> fluxes in the  
693 subtropical and subarctic North Atlantic based on measurements from a volunteer  
694 observing ship, *J. Geophys. Res.*, 111, C06024, doi:10.1029/2005JC003101, 2006.

695 [Marcello, J., Alonso, H., Eugenio, F., and Fonte, A.:](#) Seasonal and temporal study of the  
696 northwest African upwelling system, *Int. J. Remote Sens.*, 32:7, 1843-1859,  
697 doi:10.1080/01431161003631576, 2011.

698 [Mehrbach, C., Culbertson, C. H., Hawley, J. E., Pytkowicz, R. N.:](#) Measurement of the  
699 apparent dissociation constants of carbonic acid in seawater at atmospheric pressure,  
700 *Limnol. Oceanogr.*, 18, 897–907, 1973.

701 [Michaels, A. F., Karl, D. M., and Capone, D. G.:](#) Element stoichiometry, new production  
702 and nitrogen fixation, *Oceanography*, 14(4), 68–77, 2001.

703 [Mittelstaedt, E.:](#) The upwelling area off Africa—A description of phenomena related to  
704 coastal upwelling, *Prog. Oceanogr.*, 12, 307–331, doi:10.1016/0079-6611(83)90012-5.,  
705 1983.

706 **Neuer**, S., Torres-Padrón, M. E., Gelado-Caballero, M. D., Rueda, M. J., Hernández-  
707 Brito, J. J., Davenport, R., and Wefer, G.: Dust deposition pulses to the eastern subtropical  
708 North Atlantic gyre: Does ocean's biogeochemistry respond?, *Global Biogeochem.*  
709 *Cycles*, 18, GB4020, doi:10.1029/2004GB002228, 2004.

710 **Nicholson**, S. E.: Rainfall and atmospheric circulation during drought periods and wetter  
711 years in West Africa, *Monthly Weather Review*, 109(10), 2191–2208, 1981.

712 **Nightingale**, P. D., Malin, G., Law, C. S., Watson, A. J., Liss, P. S., Liddicoat, M. L.,  
713 **Boutin**, J., and **Upstill-Goddard**, R. C: In situ evaluation of air-sea gas exchange  
714 parameterizations using novel conservative and volatile tracers. *Global. Biogeochem.*  
715 *Cycles*, 14, 373-387, 2000.

716 **Nykjaer**, L., and Van Camp, L.: Seasonal and interannual variability of coastal upwelling  
717 along Northwest Africa and Portugal from 1981 to 1991, *J. Geophys. Res.*, 99, 14197–  
718 14207, 1994.

719 **Oerder**, V., Colas, F., Echevin, V., Codron, F., Tam, J., and Belmadani, A.: Peru-Chile  
720 upwelling dynamics under climate change, *J. Geophys. Res. Ocean*, 120, 1152–1172,  
721 doi:10.1002/2014JC010299, 2015.

722 **Padín**, X., Vázquez-Rodríguez, M., Castaño, M., Velo, A., Alonso-Pérez, F., Gago, J.,  
723 Gilcoto, M., Álvarez, M., Pardo, P., de La Paz, M., Rios, A. F., and Perez, F. F.: Air-Sea  
724 CO<sub>2</sub> fluxes in the Atlantic as measured during boreal spring and autumn, *Biogeosciences*,  
725 7, 1587–1606, 2010.

726 **Quan**, X. W., **Diaz**, H. F., and **Hoerling**, M. P.: Change of the Tropical Hadley Cell Since  
727 1950, In: The Hadley Circulation: Past, Present, and Future, edited by Diaz, H. F., and  
728 Bradley, R. S., , Kluwer Academic Publishers, New York, 85–120, 2004.

729 **Santana-Casiano**, J., González-Dávila, M., and Ucha, I.: Carbon dioxide fluxes in the  
730 Benguela upwelling system during winter and spring: A comparison between 2005 and  
731 2006, *Deep Sea Res. II*, 56(8), 533–541, 2009.

732 **Santana-Casiano**, J. M., González-Dávila, M., Rueda, M., Llinás, O., and González-  
733 Dávila, E- F.: The interannual variability of oceanic CO<sub>2</sub> parameters in the northeast  
734 Atlantic subtropical gyre at the ESTOC site, *Global Biogeochem. Cycles*, 21(1), GB1015,  
735 doi:10.1029/2006GB002788, 2007.

736 **Santos**, A. M. P., Kazmin, A. S., and Peliz, A.: Decadal changes in the Canary upwelling  
737 system as revealed by satellite observations: Their impact on productivity, *J. Mar. Res.*,  
738 63, 359–379, 2005.

739 Santos, F., de Castro, M., Gómez-Gesteira, M., and Alvarez, I.: Differences in coastal and  
740 oceanic SST warming rates along the Canary upwelling ecosystem from 1982 to 2010,  
741 *Continental Shelf Res.*, 47, 1-6, 2012.

742 Schuster, U., Watson, A., Bates, N., Corbiere, A., Gonzalez-Davila, M., Metzl, N.,  
743 Pierrot, D., and Santana-Casiano, J. M.: Trends in North Atlantic sea-surface fCO<sub>2</sub> from  
744 1990 to 2006, *Deep Sea Res. II*, 56(8), 620–629, 2009.

745 Takahashi, T., Olafsson, J., Goddard, J. G., Chipman, D. W., and Sutherland, S.: Seasonal  
746 variation of CO<sub>2</sub> and nutrients in the high-latitude surface oceans: A comparative study,  
747 *Glob. Biogeochem. Cycles*, 7(4), 843–878, 1993.

748 Takahashi, T., Sutherland, S., Wanninkhof, R., Sweeney, C., Feely, R., Chipman, D.,  
749 Hales, B., Friederich, G., Chavez, F., Sabine, C., Watson, A., Bakker, D., Schuster, U.,  
750 Metzl, N., Yoshikawa-Inoue, H., Ishii, M., Midorikawa, T., Nojiri, Y., Kortzinger, A.,  
751 Steinhoff, T., Hoppema, M., Olafsson, J., Arnarson, T., Tilbrook, B., Johannessen, T.,  
752 Olsen, A., Bellerby, A., Wong, C., Delille, B., Bates, N., and de Baar, H.: Climatological  
753 mean and decadal change in surface ocean pCO<sub>2</sub>, and net sea-air CO<sub>2</sub> flux over the global  
754 oceans, *Deep-Sea Res. II*, 56(8-10), 554–577, 2009.

755 Ullman, D. J., McKinley, G. A., Bennington, V., and Dutkiewicz, S.: Trends in the North  
756 Atlantic carbon sink: 1992–2006, *Glob. Biogeochem. Cycles*, 23(4),  
757 doi:10.1029/2008GB003383, 2009.

758 Varela, R., Álvarez, I., Santos, F., de Castro, M., Gómez-Gesteira, M.: Has upwelling  
759 strengthened along worldwide over 1982-2010?, *Sci. Rep.* 5, 10016;  
760 doi:10.1038/srep10016, 2015.

761 Wang, Y., Castelao, R. M., and Yuan, Y.: Seasonal variability of alongshore winds and  
762 sea surface temperature fronts in Eastern Boundary Current Systems, *J. Geophys. Res.*  
763 *Oceans*, 120, 2385–2400; doi:10.1002/2014JC010379, 2015.

764 ~~Wanninkhof, R.: Relationship between wind speed and gas exchange over the ocean, *J.*  
765 *Geophys. Res.*, 97, 7373–7382, 1992.~~

766

767 Watson, A., Schuster, U., Bakker, D., Bates, N., Corbière, A., González-Dávila, M.,  
768 Friedrich, T., Hauck, J., Heinze, C., Johannessen, T., Kortzinger, A., Metzl, N., Olafsson,  
769 J., Olsen, A., Oschlies, A., Padin, X. A., Pfeil, B., Santana-Casiano, J. M., Steinhoff, T.,  
770 Telszewski, M., Rios, A. F., Wallace, D. W., and Wanninkhof, R.: Tracking the variable  
771 North Atlantic sink for atmospheric CO<sub>2</sub>, *Science*, 326(5958), 1391–1393,  
772 doi:10.1126/science.1177394, 2009.

773 Yoo, J.-M. and Carton, J. A.: Annual and interannual variation of the freshwater budget  
774 in the tropical Atlantic Ocean and the Caribbean Sea, *J. Phys. Oceanogr.*, 20(6), 831–845,  
775 1990.  
776



777 **LEGEND FOR FIGURES**

778 Fig. 1. Ship track in the area from 28°N (Gran Canaria, The Canary Islands) to 10°N  
779 (black dots). The locations of Cap Blanc and Cape Verde are indicated. Monthly Ocean  
780 Color (oceancolor.gsfc.nasa.gov) data for average chlorophyll *a* concentration ( $\text{mg m}^{-3}$ )  
781 were included in a Matlab™ routine and annually averaged, ~~in order to draw the map~~  
782 ~~for the area~~. The map has been generated using Matlab 7.12 R2011a.

783 Fig. 2. Time series of upwelling index ( $\text{UI} \cdot 10^{-3} \text{ m}^2 \text{ s}^{-1}$ ) in the Mauritanian-Cape Verde  
784 upwelling region along the ship track computed following Nykjaer and Van Camp  
785 (1994). Cool colours are related to upwelling events and warm colours to downwelling  
786 events.

787  
788 Fig. 34. Latitudinal distribution of the interannual trends for the Upwelling Index ( $\text{UI} \cdot 10^{-3}$   
789 ) and for the four experimental variables along the QUIMA-VOS line integrated over  
790 every degree between 2005 and 2012. The a) panel presents the trends for Upwelling  
791 index ( $\text{UI} \cdot 10^{-3} \text{ m}^2 \text{ s}^{-1}$ , mean confidence interval of  $9 \text{ m}^2 \text{ s}^{-1}$ ), SST ( $^{\circ}\text{C yr}^{-1}$ , confidence  
792 interval  $0.13^{\circ}\text{C}$ ) and SSS ( $\text{yr}^{-1}$ , confidence interval 0.06) and the b) panel the trends for  
793  $f\text{CO}_2^{\text{sw}}$  and  $f\text{CO}_2^{\text{atm}}$  (confidence intervals  $4.23 \mu\text{atm}$  and  $0.44 \mu\text{atm}$ ).

794  
795 Fig. 43. In situ data of a) SST and b) SSS data in the Mauritanian - Cape Verde coastal  
796 region grouped by seasons: winter (W, December, January and February), spring (Sp,  
797 March, April and May), summer (Sm, June, July and August) and autumn (Au,  
798 September, October and November). The averaged values for all cruises in Table S1, are  
799 shown in black for each season including the 95% confidence limits. Colour code for each  
800 cruise is that indicated in Table S1.

801

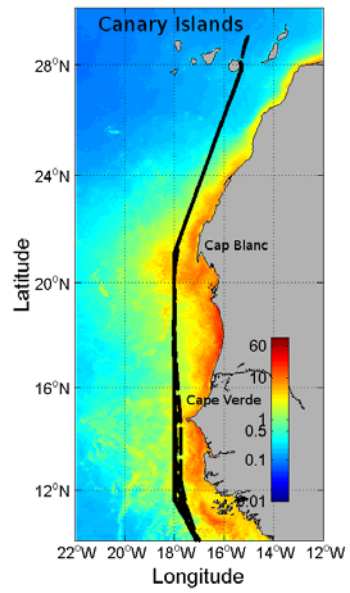
802 Fig 5. fugacity of CO<sub>2</sub> data in the Mauritanian-Cape Verde coastal region grouped by  
803 seasons: winter (W), spring (Sp), summer (Sm) and autumn (Au). a)  $f\text{CO}_2^{\text{sw}}$  latitudinal  
804 distribution. b) Difference between measured and Normalized  $f\text{CO}_2^{\text{sw}}$  values to a constant  
805 temperature of 22°C. The averaged values for all cruises in Table S1, are shown in black  
806 for each season including the 95% confidence limits. Colour code for each cruise is that  
807 indicated in Table S1.

808 Fig. 6. pH at *in situ* SST in total proton scale computed from total alkalinity (based on  
809 regional correlations with SST and SSS, Lee et al., 2006) and  $f\text{CO}_2$  at  $21 \pm 0.25$  °N. The  
810 error bar represents the standard deviation of the computed data for each cruise for the  
811 selected latitude. The black line shows the harmonic fitting Eq. (4) for the data and the  
812 corresponding linear trend.

813 Fig. 7. Latitudinal distribution of seasonal and annual CO<sub>2</sub> fluxes,  $\text{FCO}_2$  ( $\text{mol m}^{-2}$ ). Fluxes  
814 of CO<sub>2</sub> were computed using Nightingale et al. (2000) parametrization and satellite winds  
815 with a resolution of 6 hours. a) Integrated year-to-year from 2005 to 2012 and b)  
816 latitudinally integrated for 2005 to 2012 together with annual values for NAO index.  
817 Latitudinal distribution of  $\text{FCO}_2$  seasonally integrated from 2005 to 2012 are depicted for  
818 winter (c, December, January and February), spring (d, March, April and May), summer  
819 (e, June, July and August) and autumn (f, September, October and November).

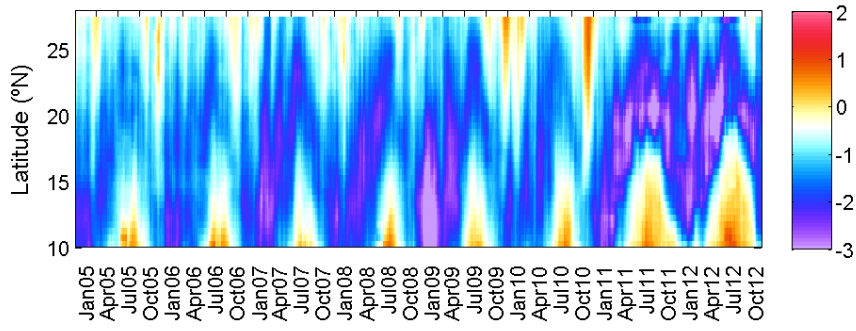
820

821 Fig. 1



822

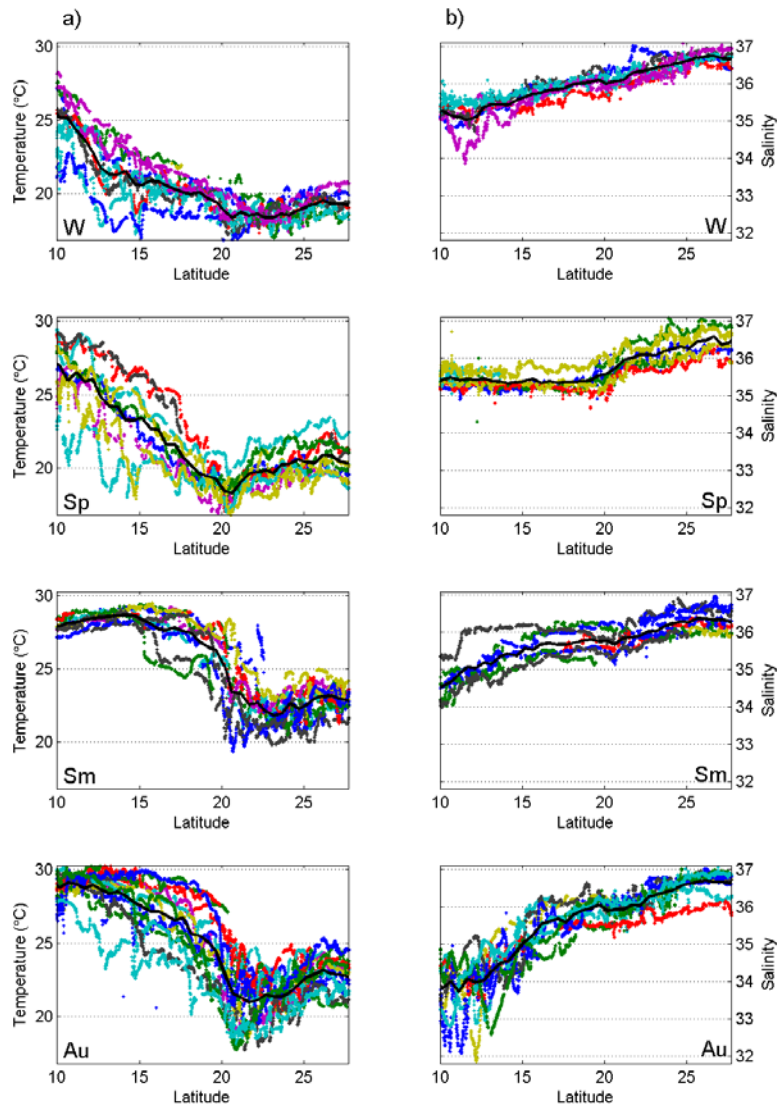
823 Fig. 2



824  
825

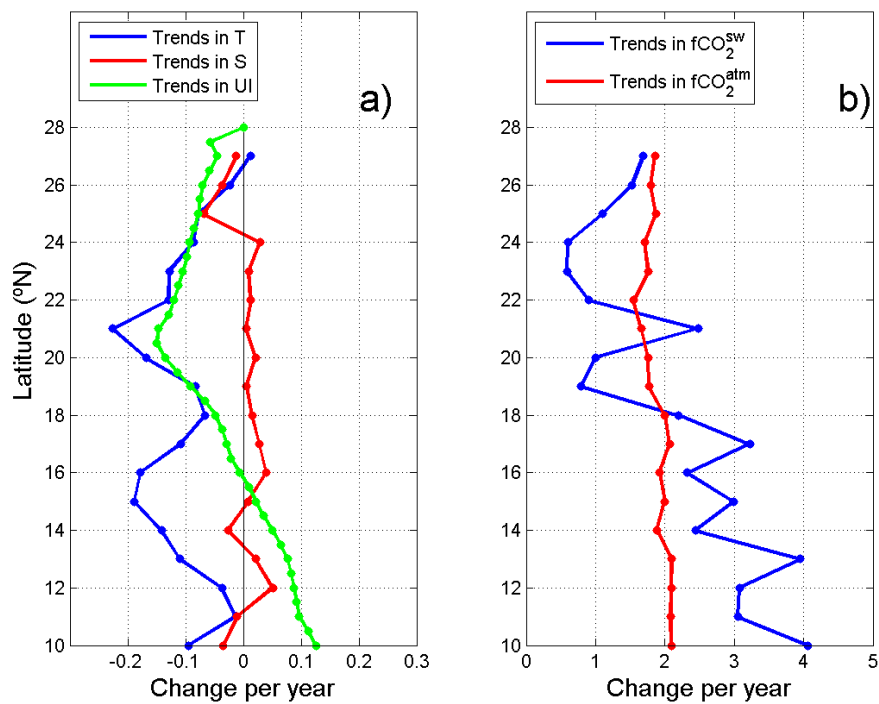
826  
827  
828

Fig. 34



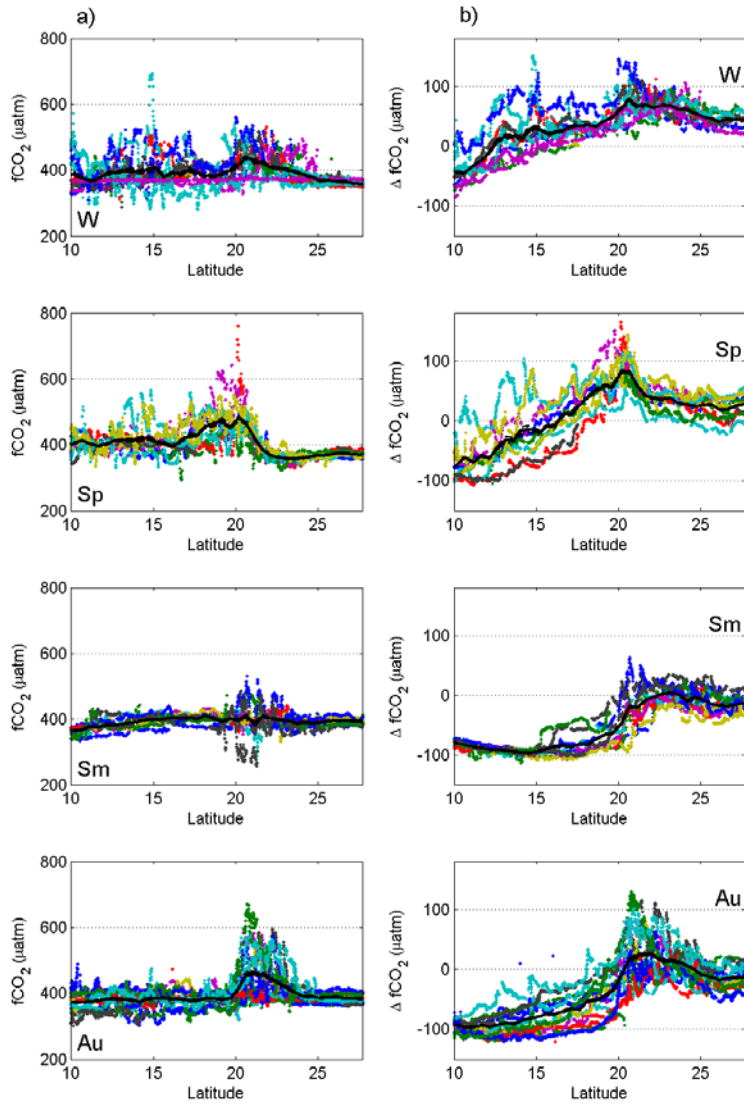
829  
830  
831

832 Fig. 4  
833



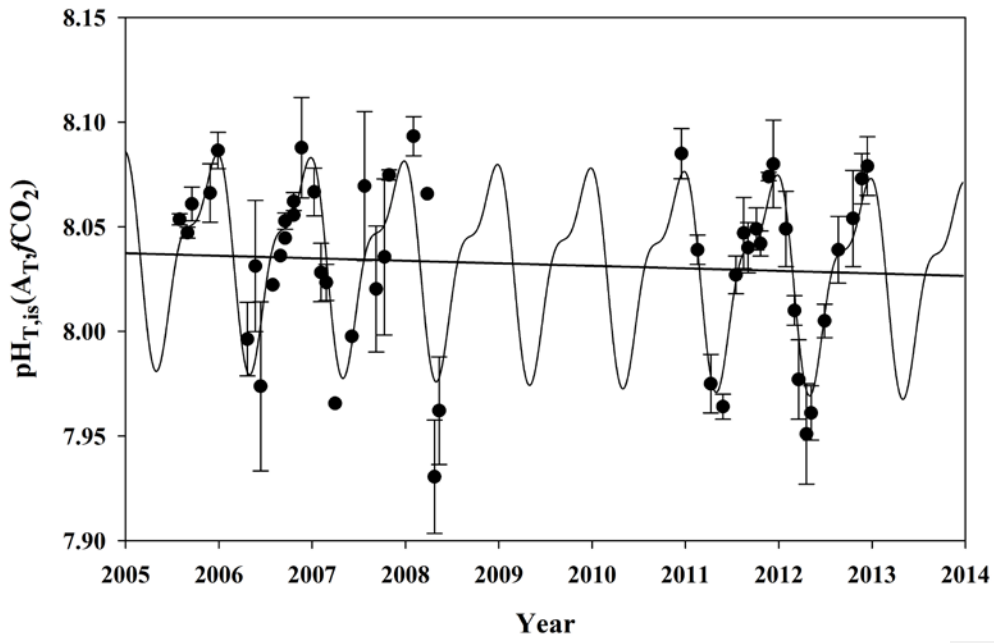
834

835 Fig. 5



836  
837

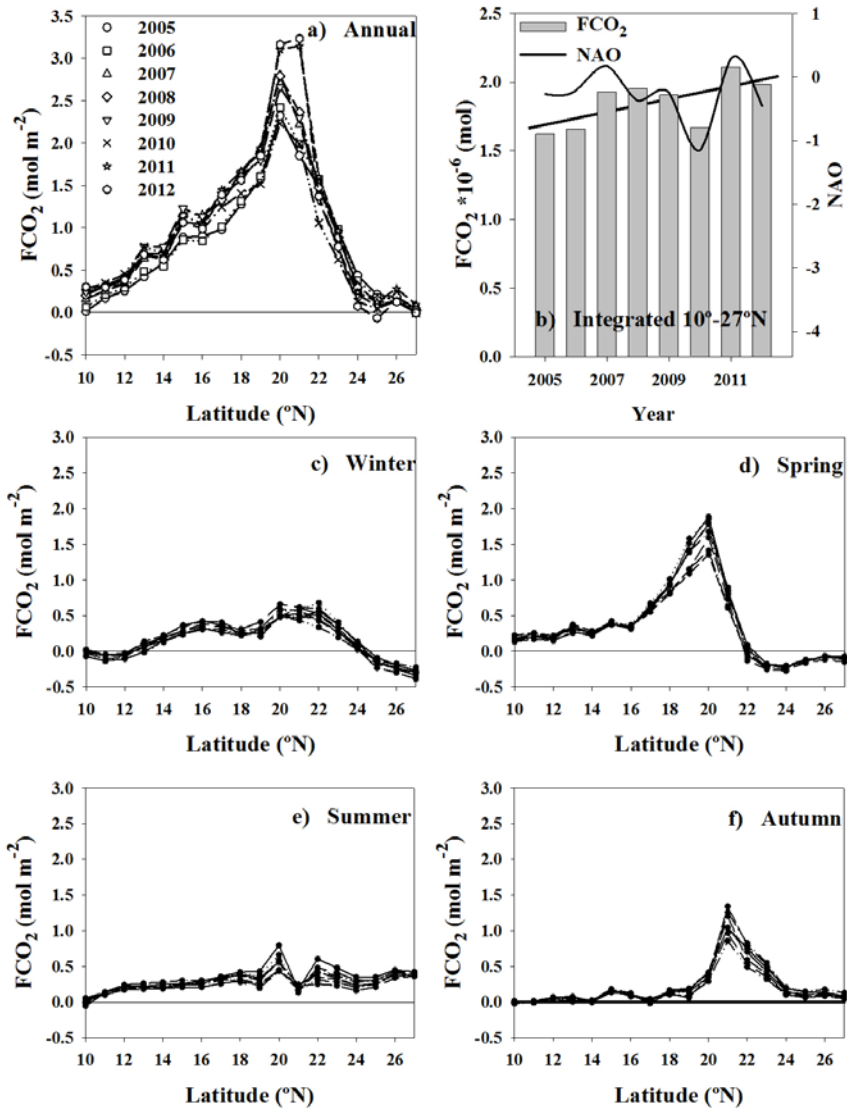
838 Fig. 6



839  
840



841 Fig. 7



842  
843